Quantum theory of local perturbation of the charge-density wave by an impurity: Friedel oscillations

I. Tüttő and A. Zawadowski
Central Research Institute for Physics, Hungarian Academy of Sciences, P.O. Box 49, H-1525 Budapest 114, Hungary
(Received 22 October 1984)

The interaction of a single impurity with a charge-density wave (CDW) cannot be described by Ginzburg-Landau theory. In the present paper a one-dimensional microscopic quantum theory is presented considering only the backward scattering of the electrons by the impurity at zero temperature. This theory considers the strong perturbation of the CDW inside the amplitude coherence length, which perturbation is dominated by the Friedel oscillations at short distances. It treats the CDW within the framework of the mean-field approximation, and sums up the backward scattering to all orders in perturbation theory. The main features of a self-consistent treatment of the mean field is briefly outlined and the modification can be embodied into the renormalization of the impurity scattering. The results obtained are sensitive to the impurity-scattering strength. In first order, the results of the rigid CDW are reproduced; in second order, the previous results by Barnes and Zawadowski are obtained. The largest effects are in the strong-scattering region. The following physical quantities are calculated: electron density, ground-state energy, density of states, and the force exerted by the impurity on the CDW as a function of the relative position of the impurity with respect to the CDW, and a solution of the equation of motion is found. Considering the electron density in the intermediate-coupling-strength case, the Friedel oscillations dominate at short distances well inside the amplitude coherence length. In the charge density, the Friedel oscillations and the CDW are additive to a good approximation. Outside the amplitude coherence length, the Friedel oscillations tunnel into the CDW gap. In the density of states at the impurity site, the singularity at the gap edge is smeared out and a pair of bound states appears in the gap if the CDW and the Friedel oscillations are out of phase. Further bound states appear also outside the conduction band. The effective potential describing the interaction of the CDW with the impurity is very nonsinusoidal in the intermediate-coupling-strength region, but becomes more sinusoidal for very weak and very strong coupling. The effect of this nonsinusoidal potential in the equation of motion is in the enhancement of higher harmonics appearing in the narrow-band noise, but their intensities remain monotonically decreasing. Among the observable effects predicted are the following: the temperature dependence of the ratios of the intensities of the harmonics in the narrow-band noise, the effect of the nonsinusoidal potential in the Shapiro steps, and the appearance of Friedel oscillations in NMR and diffraction experiments.

I. INTRODUCTION

Thirty years ago Fröhlich[1] proposed the charge density wave (CDW) state as a candidate for carrying coherent current on macroscopic scale, however, strong experimental evidences for that idea appeared in the literature only in the last few years. The first material in which the sliding in an incommensurate CDW has been observed is $NbSe_3$.[2] The crucial experimental discoveries that have been made are the nonohmic conductivity with a critical electric field (threshold field) which must be exceeded to have the CDW sliding,[2] and the narrow band noise,[3] which means an ac response for dc applied voltage. For more experimental details we refer to the excellent review articles that have appeared in the literature (see Ref. 4). Most of the theoretical approaches are classical, namely, the CDW is considered as a rigid object[5,6] moving in a periodic potential[7] with periodicity equal to the wave length of the CDW, or a deformable medium[8–10] described by the classical theory of elasticity. The latter is essentially a Ginzburg-Landau theory where only the phase of the CDW is deformed but its amplitude is taken unchanged. In all of these theories the pinning of the CDW by impurities is manifested in the threshold field. For a long period of time, the only quantum approach to the problem had been proposed by Bardeen,[11,12] who suggested that tunneling in the vicinities of the impurities is responsible for the weak coupling between two macroscopic quantum states. Recently, Barnes and Zawadowski[13] have proposed that the weak scattering on impurities may result in a weak coupling between the two quantum states corresponding to the right and left moving CDW states. In this sense their theory shows a strong resemblance to Bardeen's theory,[11,12] but without the idea of Zener tunneling. This theory exhibits also a strong formal analogy with the theory of Josephson junctions. There are several other approaches as well, e.g., where smaller commensurate regions are separated by transition regions of the soliton type.[14] Some recent experiments have been interpreted as direct evidence for the generation of the narrow-band noise by the regions of the electric contacts.[15] The relevant theories are based on formations

 ©1985 The American Physical Society

of vortices[15] or phase slip centers[16] near the contacts.

The present work is an extension of the theory of Barnes and Zawadowski[13] and based on the physical ideas summarized in Ref. 17. In the previous work,[13] the analogy with the Josephson junction is emphasized, this treatment is focused, however, on the amplitude and phase perturbation of the CDW in the immediate vicinity of a single impurity. The present study is motivated by several theoretical and experimental problems.

Considering the theoretical problems, the following are the most important.

(i) In the classical model where the CDW is treated as a single particle, any internal motion or deformation of the CDW is completely ignored.

(ii) The Efetov-Larkin[8] and the Fukuyama-Lee-Rice[9] theory of the CDW is capable of describing the long-range deformation but certainly does not deal with any perturbation on a length scale shorter than the amplitude coherence length $\xi_0=v_F/\Delta_0$ where v_F is the Fermi velocity and Δ_0 is the gap characterizing the CDW.

(iii) The microscopic processes have been recently considered by Barnes and Zawadowski[13] to second order in the backward scattering on the impurity. The higher-order processes, however, have not been considered; therefore, the physical relevance of those calculations has remained somewhat in doubt.

(iv) Friedel oscillations[18] must occur in the conduction-electron density around an impurity in any metal. As the CDW gap is small this oscillation must exist in the CDW state as well. As both the periodicity distance of the Friedel oscillation and the wavelength λ of the CDW are determined by twice the Fermi momentum k_F, therefore, a strong interaction and competition between the CDW and the Friedel oscillation is expected around the impurity.

From the point of view of the experiments the following questions are related to the present work.

(i) Does the effective potential, by which the interaction between the impurity and the CDW and the phenomenological taken into account, have a sinusoidal form or is there a strong deviation from that?

(ii) Is λ or $\lambda/2$ the periodicity of that effective potential as has been suggested by Monceau *et al.*?[19]

(iii) Do the ratios of the harmonics in the narrow-band noise depend on the temperature or not?

(iv) Does the magnetic interaction with magnetic impurities contribute to the pinning of the CDW or not?

The role of magnetic impurities has been recently studied experimentally[20] and a theory has been worked out considering the Josephson-type processes[21] to second order in the magnetic exchange coupling. The extension of this theory is, however, beyond the scope of the present paper.

Concerning the theoretical motivations (iii) and (iv), further remarks will be made.

The CDW phase is characterized by the formation of electron-hole bound pairs with total momentum $\pm Q$ and with total spin $S=0$ ($Q=2\pi/\lambda$). There are two different types of pairs with momenta $\pm Q$, respectively, which are condensed forming two macroscopic quantum states (see Fig. 1). The interference between the left- and right-going condensate results in the formation of the CDW. The

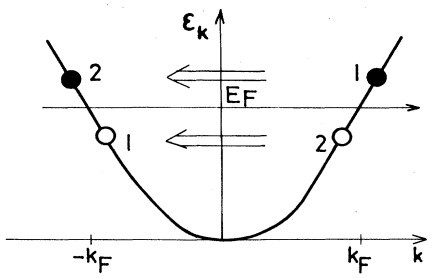

FIG. 1. 1D dispersion curve with the two types of electron-hole pairs (labeled by 1 and 2) forming the CDW. The arrows are indicating the two backscatterings on the impurity which represent a transition between the different pairs.

second-order term in the acceleration of the CDW due to a single impurity calculated by Barnes and Zawadowski[13] corresponds to the transition of two electrons from the same side of the dispersion curve to the opposite one by backward scatterings at the impurity. Thus, this process contributes to the transition between the two different types of pair (see Fig. 1). The right- (left-) going pairs are characterized by the macroscopic phase $-\varphi$ ($+\varphi$). The phase φ also determines the position of the CDW. The rate of the pair transitions is proportional to $\sin[2(\varphi-\varphi_0)]$, where the phase φ_0 is determined by the position of the impurity. Thus, the position of the CDW with respect of the impurity determines whether the number of right- or left-going pairs increases in this scattering process, or in other words, whether the acceleration of the CDW due to the impurity is in the right or left direction. In the case of a CDW moving with constant velocity the phase φ of the CDW varies monotonically, thus the acceleration and the transition rate oscillate in time. There is, however, a difference between the present case and the Josephson junction, because the two condensates of the CDW are located in the same volume, just as in the case of superfluid He_3 where the pairs show the Leggett oscillation in the presence of an external magnetic field.[22] There is another difference, namely, the third order in perturbation theory gives a finite contribution to the acceleration of the CDW, in contrast to the Josephson effect. The origin of this difference is that the electrons move in an effective periodic potential induced by the CDW and the scattering on that results also in backscattering with momentum transfer $\pm Q$. Thus, e.g., a transition of an electron from right to left may occur as two right-left scatterings on the impurity and a left-right scattering on this effective periodic potential, which transition is the second of the processes depicted in Fig. 2. In the mathematical sense, the scattering due to the effective potential appears as the anomalous left-right (right-left) Green's function[23] G_{LR} (G_{RL}) and the process is described as

$$TG_{LR}T\ , \tag{1.1}$$

which is the first correction to the backscattering amplitude T.

The motivation concerning the Friedel oscillation deserves also a longer discussion. The electron density

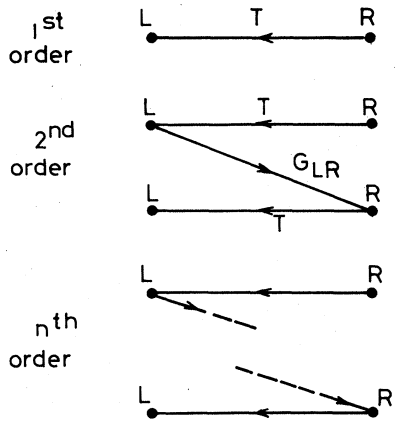

FIG. 2. Diagrammatic representation of the scattering of an electron from right to left in the perturbation theory.

around an impurity is shown schematically in Fig. 3. At the impurity the electrons are affected by the impurity potential which has a height of about 0.1—1 eV depending upon whether the impurity is weak (neutral) or strong (charged).[8] Furthermore, the electrons move in the mean field potential due to the CDW which has the amplitude of the CDW gap $\Delta_0 \sim 0.01$ eV. Since at the impurity site the effect of the impurity is the dominant one, the Friedel oscillation must be formed around the impurity. If the height of the impurity potential is comparable with the bandwidth D then the amplitude of the Friedel oscillations approaches the total electron density in the band. Because of the large damping of the Friedel oscillations at larger distances measured from the impurity, there exists a crossover distance x_0 beyond which the CDW dominates the Friedel oscillation. The main phenomena is that the impurity tries to lock the phase of the oscillation in order to have the maximal or minimal electron density at the impurity depending on the sign of the impurity potential. In general this locking phase is different from the phase φ of the unperturbed CDW; thus these two different phases must be matched in the crossover region around x_0.

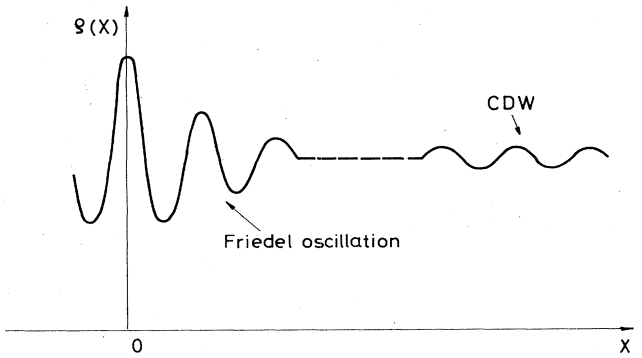

FIG. 3. Schematic plot of the electron density around an impurity. The region of mismatch between the regions dominated by Friedel oscillations and by CDW is represented by the dotted line.

The picture of the interaction between the sliding CDW and the impurity is very different from that in Ginzburg-Landau theory, in which the phase $\varphi(x)$ of the CDW is a slowly varying function of the space coordinate x, and that phase determines the electron density at the impurity site which interacts locally with the impurity. In the present theory, if the impurity is strong, then the phase of the CDW is locked at the impurity and the interference between the Friedel oscillation and the CDW determines the interaction energy and the force F exerted on the CDW by the impurity. It must be emphasized that the Friedel oscillation is dominant over a few atomic distances (a) around the impurity, while the phase of the CDW is slowly varying on the length scale of the amplitude coherence length ξ_0. In most of the case $\xi_0 \gg x_0$, thus the phase of the CDW cannot be very different on the two different sides of the impurity just beyond the crossover region ($x_0 < x < \xi_0$). In the present theory the interaction with the impurity is treated in perturbation theory. It will be shown that this theory provides the modification of the CDW only in the intermediate vicinity of the impurity $x < \xi_0$ and does not produce the long-range phase deformation of the CDW. In a realistic case, the long-range deformation acts to minimize the mismatch of the phase in the crossover region. In the case of a single impurity in an infinitely long sample, the mismatch always disappears due to the long-range deformations, but that is not the case in the presence of many impurities. Thus the present theory gives the correct deformation of the CDW on very short length scales $x < \xi_0$ only. The long-range deformation is beyond the scope of the present paper and that must be obtained from the Ginzburg-Landau theory,[8,9] where the CDW impurity interaction is taken from the present theory. The Fukuyama-Lee-Rice theory[8,9] of that type provides the long-range phase coherence length ξ known as the Lee-Rice length ($\xi \gg \xi_0$ for weak impurities).

The basic scheme of the formalism applied in the present paper is as follows. The interaction leading to the CDW is treated in the mean field approximation and the perturbation by the impurity is treated in the same manner. First the mean field is taken from the case without impurities and later the main features of a self-consistent theory are briefly outlined. It will be shown that the qualitative picture presented is not affected by taking the mean field of the impurity-free case.

The high degree of anisotropy of the conductivity and the structural data support that these type of materials such as $NbSe_3$ are quasi-one-dimensional. Instead of using the realistic, but very complicated Fermi surface, it is widely accepted to adopt a model with a Fermi surface consisting of two almost-parallel planes. The role of the nesting of these planes was discussed in details by Gor'kov and Dolgov,[24] who have shown that the one-dimensional model leads to a qualitatively correct picture in a mean field approximation. The shortcomings of the one-dimensional model are the lack of the extension of the perturbation in the perpendicular directions. In our problem the extension of the Friedel oscillations in perpendicular directions depends on the interchain coupling. The

region of the Friedel oscillations around the impurity has a cigar shape. The behavior, however, in the longitudinal direction is effected only slightly. In this paper for the sake of simplicity a strictly one dimensional problem is treated in the mean field approximation keeping in mind that in reality the Friedel oscillations are three dimensional.

Therefore the model to be treated is strictly one-dimensional and for sake of simplicity only the backward scattering on the impurity is treated.

In Sec. II the formalism is presented. Section III is devoted to the calculations of the electron density and the order parameter at the impurity site and to the ground-state energy. In Sec. IV, the electron density is obtained at finite distance. Section V contains the result for the density of states and for the bound electron states which may appear as has first been pointed out by Gor'kov and Dorokhov.[25] In Sec. VI the force exerted on the CDW by the impurity is calculated as the derivative of the interaction energy with respect of the position of the CDW. The single particle model for the moving CDW is discussed in Sec. VII with the force derived in Sec. VI. In the Conclusion the experimental consequences of the present theory are briefly summarized. Appendices A and B are devoted to the calculation of the CDW acceleration in third order of perturbation theory using the real time technique in order to check the validity of the simpler method of Sec. VI. The formalism of the wave function of BCS-type is quoted in Appendix A and applied in Appendix B. Finally, in Appendix C the self-consistent theory is outlined.

II. FORMALISM

The Hamiltonian H to be treated consists of the Hamiltonian $H_{\rm el}$ of the interacting electron gas forming the CDW and of $H_{\rm imp}$ describing the interaction between electrons and a single impurity,

$$H=H_{\rm el}+H_{\rm imp}\ . \tag{2.1}$$

The part $H_{\rm el}$ must contain the kinetic energy of electrons and the interaction responsible for the formation of the CDW which may be a direct electron-electron interaction or electron-phonon interaction. In the latter case $H_{\rm el}$ includes the phonon part as well. The formation of the CDW without the impurity will be treated in the mean-field approximation, which can be formulated either by using the anomalous Green's functions introduced by Gor'kov or by introducing a BCS-type ground-state wave function and quasiparticle operators following the Bogolyubov formalism applied to superconductivity (for the latter see Appendix A). In the mean-field approximation, the interaction is embodied into the uniform gap "field" $\Delta_0(\varphi)=\Delta_0 e^{i\varphi}$, with phase φ and an effective Hamiltonian $H_{\rm CDW}$ can be introduced,

$$H_{\rm CDW}=\sum_{k,\sigma}\epsilon_k a^\dagger_{k,\sigma}a_{k,\sigma} + \left[\Delta_0(\varphi)\sum_{p,\sigma}a^\dagger_{p+Q/2,\sigma}a_{p-Q/2,\sigma}+\text{c.c.}\right], \tag{2.2}$$

where $a^\dagger_{k\sigma}$ and $a_{k\sigma}$ are the free-electron creation and annihilation operators in one dimension, $\epsilon_k=v_F(|k|-k_F)$ is the kinetic energy linearized near the Fermi momenta $\pm k_F$, v_F is the Fermi velocity, Q is the wave vector of the CDW ($Q=2k_F$), and for the momentum p, a symmetrical cutoff $p_0=D/v_F$ is applied, where the energy D is of the order of the bandwidth. That approximate dispersion curve is depicted in Fig. 4.

One of the most important approximations to be applied is that Δ_0 is taken to be uniform and not affected by the presence of the impurity. In a self-consistent approximation, the change $\delta\Delta(x)=\Delta(x)-\Delta_0(\varphi)$ due to the impurity must be fed back into Eq. (2.2). The Green's functions are, however, sensitive to an appropriate space average of $\delta\Delta(x)$ taken over a region which has a characteristic size of the amplitude coherence length known as the BCS length $\xi_0=v_F/\Delta_0$. As will be seen, $\delta\Delta(x)/\Delta_0$ is relatively large only in the intermediate vicinity of the impurity (few atomic distances), which is a region small compared to ξ, thus the change $\delta\Delta(r)$ can be taken into account by a weak renormalization of the impurity scattering as will be shown in Appendix C.

In the mean-field approximation the definition of the energy gap $\Delta_0(\varphi)$, the quasiparticle energy $E(k)$, and the gap equation are of the BCS type; thus

$$\Delta_0(\varphi)=g\sum_{p,\sigma}\langle a^\dagger_{p-Q/2,\sigma}a_{p+Q/2,\sigma}\rangle\ , \tag{2.3}$$

and

$$E_p=E(k)=[\Delta_0^2+(v_F p)^2]^{1/2}\ , \tag{2.4}$$

where $k=\pm Q/2+p$ and

$$1=-gs\sum_p\frac{1}{2E_p}\ , \tag{2.5}$$

which gives for Δ_0

$$\Delta_0=D\left[\sinh\left[\frac{2\pi v_F}{|g|s}\right]\right]^{-1}\approx 2D\exp\left[-\frac{2\pi v_F}{|g|s}\right], \tag{2.6}$$

where the effective electron-electron coupling $g<0$ includes the phonon exchange, D is the symmetric bandwidth cutoff, and s is the degree of spin degeneracy (in the real case $s=2$), otherwise the spin index will be dropped in the paper.

In the usual way the electron field operator can be split

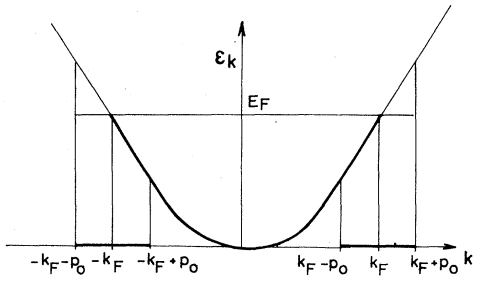

FIG. 4. 1D dispersion curve. Only those electrons with momenta p are taken into account in our model, for which holds $k_F-p_0<|p|<k_F+p_0$.

into left (L) and right (R) moving parts,[13,26]

$$\psi(x)=\psi_L(x)+\psi_R(x) , \tag{2.7}$$

with

$$\psi_\alpha(x)=\frac{1}{L^{1/2}}\sum_{\alpha k\,(>0)} e^{ikr}a_k \quad \text{with} \quad \alpha=R,L , \tag{2.8}$$

where L is the length of the system and $\alpha=\pm 1$ on the right-hand side of Eq. (2.8) stands for the right (R) and left (L), respectively. Considering an incommensurate CDW (no umklapp processes) without impurities the number of left and right electrons are conserved; thus the following two quantities are conserved,[13]

$$N_\alpha=\int dx\,\psi_\alpha^\dagger(x)\psi_\alpha(x), \quad \alpha=L,R . \tag{2.9}$$

This conservation law can be manifested by the following gauge transformation

$$\psi_\alpha\rightarrow\psi_\alpha e^{i\varphi_\alpha} \tag{2.10}$$

where φ_L and φ_R are arbitrary phases. The difference $\varphi=\varphi_L-\varphi_R$ is associated with the real-space position of the degenerate ground state of the CDW. Thus, the total electron density $\rho^0(x)$ at position x is (see Appendix A)

$$\rho^{(0)}(x)=s\langle\psi^\dagger(x)\psi(x)\rangle=s[\rho_0-\rho_1\cos(Qx-\varphi)] , \tag{2.11}$$

with

$$\rho_0=\frac{D}{\pi v_F} , \tag{2.12}$$

and

$$\rho_1=\frac{\Delta_0}{s\pi v_F\hat{g}} , \tag{2.13}$$

where ρ_0 is the average electron density for one spin direction and ρ_1 is the amplitude of the CDW and the dimensionless coupling is $\hat{g}=-g/2\pi v_F$. Furthermore, the phase of the gap is given as

$$\Delta_0(x)=\Delta_0 e^{i(Qx-\varphi)} . \tag{2.14}$$

In Eq. (2.11), ρ_0 is determined by $\langle\psi_R^\dagger\psi_R\rangle$ and $\langle\psi_L^\dagger\psi_L\rangle$, while the cross terms $\langle\psi_R^\dagger\psi_L\rangle$ and $\langle\psi_L^\dagger\psi_R\rangle$ contribute to ρ_1.

In order to study the role of impurities, one can consider the most simple interaction Hamiltonian H_1,

$$H_1=V\sum_{R_i}\psi^\dagger(R_i)\psi(R_i) , \tag{2.15}$$

where V is the local electron-impurity interaction potential and R_i is the position of the impurity "i". In the general case V may depend on the momentum transfer q, and the values $V(q\approx 0)$ and $V(q\approx\pm Q)$ are of importance. The calculation can be simplified if the forward scattering $V(q=0)$ is dropped and only the backward scattering $T=V(q=\pm Q)$ is kept, which of course is a strong limitation. Thus, in this case the Hamiltonian for a single impurity located at the origin has the form

$$H_{\rm imp}=T[\psi_R^\dagger(0)\psi_L(0)+\psi_L^\dagger(0)\psi_R(0)] . \tag{2.16}$$

This Hamiltonian does not show the gauge invariance given by Eq. (2.10); thus the ground state is not degenerate any more as the impurity can pin the CDW in a preferable position. It follows also from the gauge transformation that any result obtained for $\varphi=0$ can be generalized for a CDW with arbitrary position (given by φ) by the substitutions $T\rightarrow Te^{+i\varphi}$ and $T\rightarrow Te^{-i\varphi}$ in the first and second terms in the right-hand side of Eq. (2.16), respectively.

Although our calculation will be valid only at zero temperature, for convenience, the finite-temperature Green's function will be applied and the zero-temperature limit [$\beta=(k_BT)^{-1}\rightarrow\infty$] will be taken afterward.

The definition of the Green's function including the effect of impurities is

$$G_{\alpha\beta}(x,x';\tau-\tau')=-\langle T_\tau\{\psi_\alpha(x,\tau)\psi_\beta^\dagger(x',\tau')\}\rangle , \tag{2.17}$$

where τ is the complex time variable (see, e.g., Ref. 27).

Following the real-space technique of Ref. 26, the Green's function without impurities can be written in the form

$$G_{\alpha\beta}^{(0)}(x,x';\tau-\tau') = e^{i[(Q/2)(\alpha x-\beta x')+\varphi_\alpha-\varphi_\beta]}\hat{G}_{\alpha\beta}^{(0)}(x-x',\tau-\tau') , \tag{2.18}$$

where $\hat{G}_{\alpha\beta}^{(0)}$ depends only on the differences of the arguments, and it is independent of the gauge; thus its Fourier transform can be written as

$$\hat{G}_{\alpha\beta}^{(0)}(x-x',\tau-\tau') =\frac{1}{\beta}\sum_{p,\omega_n} e^{i[p(x-x')-\omega_n(\tau-\tau')]}\hat{G}_{\alpha\beta}(p,i\omega_n) , \tag{2.19}$$

where $\omega_n=(2n+1)\pi\beta^{-1}$ and $-p_0<p<p_0$ ($p_0<k_F$). Furthermore

$$\hat{G}_{RR}^{(0)}(p,i\omega_n)=\hat{G}_{LL}^{(0)}(-p,i\omega_n) =\frac{1}{2}\left[\frac{1+(v_Fp/E_p)}{i\omega_n-E_p}+\frac{1-(v_Fp/E_p)}{i\omega_n+E_p}\right] , \tag{2.20}$$

and

$$\hat{G}_{LR}^{(0)}(p,i\omega_n)=\hat{G}_{RL}^{(0)}(p,i\omega_n) =\frac{\Delta_0}{2E_p}\left[\frac{1}{i\omega_n-E_p}-\frac{1}{i\omega_n+E_p}\right] \tag{2.21}$$

(see, e.g., Ref. 23).

The main part of the paper is devoted to calculating the effect of the impurities on the total electron density $\rho(x)$ at position x, the gap $\Delta(x)$, and the change in the thermodynamical potential Ω. These quantities are given as follows:

$$\rho(x)=s\sum_{\alpha,\beta=L,R}G_{\alpha\beta}(x,x;\tau\rightarrow-0) , \tag{2.22}$$

and

$$\Delta(x)=\mathrm{sgn}G_{RL}(x,x;\tau\rightarrow-0) , \tag{2.23}$$

and

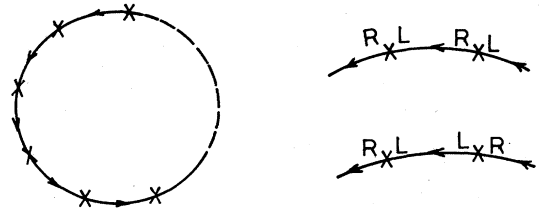

FIG. 5. Typical ring diagram for the perturbation expansion of the thermodynamical potential. The crosses represent the electron impurity scattering process. Typical sections of the ring diagrams are also shown.

$$\delta\Omega = \int_0^T dT' \frac{1}{T'} \langle H_{\rm imp}(T') \rangle \tag{2.24}$$

(see, e.g., Ref. 26).

The later expression can be rewritten by using Eqs. (2.16) and (2.17),

$$\delta\Omega = s \int_0^T dT' \lim_{\tau \to 0} [G_{RL}(0,0;\tau) + G_{LR}(0,0;\tau)]_{T'} . \tag{2.25}$$

This simple form of the thermodynamical potential is due to the fact that the interaction $H_{\rm int}$ contains only two fermion operators. Thus the present calculation of the thermodynamical potential corresponds to the summation of the ring diagrams depicted in Fig. 5, where the lines connecting the crosses representing the interaction with the impurities correspond to normal or anomalous Green's functions ($G^{(0)}_{\alpha\beta}$). Typical sections of the ring are also shown in Fig. 5. The actual calculations of the quantities presented here are the subject of the next section.

III. PERTURBATION THEORY FOR THE ELECTRON DENSITY AND THE ORDER PARAMETER AT THE IMPURITY SITE AND FOR THE GROUND-STATE ENERGY

The first step is to consider the effect of the impurity on the Green's function. The Dyson equation for the Green's function (2.17) with interaction (2.16) can be given in a matrix form,

$$G_{\alpha\beta}(x,x';i\omega_n) = G^{(0)}_{\alpha\beta}(x,x';i\omega_n) + G^{(0)}_{\alpha\gamma}(x,0;i\omega_n) t_{\gamma\delta} G_{\delta\beta}(0,x';i\omega_n) , \tag{3.1}$$

where for backward scattering t is off-diagonal $t_{\gamma\delta} = T\delta_{\gamma,-\delta}$ and summation is applied over the indices occurring twice. The summation of the perturbation series can be carried out exactly, because only $G_{\alpha\beta}(0,0;i\omega_n)$ appears in the intermediate steps. The general dependence of $G_{\alpha\beta}(x,x';i\omega_n)$ on x and x', however, cannot be given in a closed algebraic form. Thus we solve first the case $x = x' = 0$ and we use that result to calculate $\delta\Omega$ by applying Eq. (2.25).

The solution of the Dyson equation (3.2) for $G_{\alpha\beta}(0,0;i\omega_n)$ may be written in the following matrix:

$$[G(0,0;i\omega_n)]_{\alpha\beta} = \frac{1}{d(i\omega_n)} \begin{bmatrix} G^{(0)}_{RR} & G^{(0)}_{RL} - T(G^{(0)}_{RL}G^{(0)}_{LR} - G^{(0)}_{RR}G^{(0)}_{LL}) \\ G^{(0)}_{LR} - T(G^{(0)}_{LR}G^{(0)}_{RL} - G^{(0)}_{LL}G^{(0)}_{RR}) & G^{(0)}_{LL} \end{bmatrix}_{x=x'=0,\, i\omega_n} , \tag{3.2}$$

where

$$d(i\omega_n) = 1 - T(G^{(0)}_{LR} + G^{(0)}_{RL})_{x=x'=0,\, i\omega_n} + T^2(G^{(0)}_{LR}G^{(0)}_{RL} - G^{(0)}_{LL}G^{(0)}_{RR})_{x=x'=0,\, i\omega_n} . \tag{3.3}$$

The unperturbed Green's function can be calculated by integrating Eqs. (2.19), (2.20), and (2.21) with respect to the momentum. Thus, one obtains

$$G^{(0)}_{RR}(0,0;i\omega_n) = G^{(0)}_{LL}(0,0;i\omega_n) = -\frac{i\omega_n}{2v_F(\omega_n^2 + \Delta_0^2)^{1/2}} C(\omega_n) , \tag{3.4}$$

and

$$G^{(0)}_{LR}(0,0;i\omega_n) = [G^{(0)}_{RL}(0,0;i\omega_n)]^* = -\frac{\Delta_0}{2v_F(\omega_n^2 + \Delta_0^2)^{1/2}} e^{i\varphi} C(\omega_n) , \tag{3.5}$$

where

$$C(\omega_n) = \frac{2}{\pi} \arctan \frac{D}{(\omega_n^2 + \Delta_0^2)^{1/2}} , \tag{3.6}$$

which reproduce the results of Ref. 26 in the limit $D \to \infty$.

In the calculations of the different physical quantities at finite temperature, it would be a very difficult task to perform the energy sums. Therefore, the present work is restricted to the zero temperature case. In this case ($\beta \to \infty$) the sum is replaced by the integral as

$$\frac{1}{\beta} \sum_n \to \frac{1}{2\pi} \int_{-\infty}^{\infty} d\omega . \tag{3.7}$$

First we calculate three quantities which occur in Eqs. (2.22)–(2.25). Using Eq. (3.4), the well-known calculation provides

$$\lim_{\tau \to -0} G^{(0)}_{\alpha\alpha}(0,0;\tau) = \lim_{\tau \to -0} \frac{1}{2\pi} \int d\omega\, e^{-i\omega\tau} G^{(0)}_{\alpha\alpha}(0,0;i\omega) d\omega = \frac{D}{2\pi v_F} = \frac{\rho_0}{2} \quad (\alpha = R,L) , \tag{3.8}$$

where ρ_0 defined by Eq. (2.12) is the unrenormalized electron density which is not affected by the interaction leading to the formation of the CDW.

Considering the difference $\lim_{\tau \to -0} [G_{\alpha\alpha}(0,0,\tau) - G^{(0)}_{\alpha\alpha}(0,0,\tau)]$, one can set $\tau = 0$, as that quantity can be transformed to an integral with respect to ω and the integrand behaves as ω^{-2} at large energies. Furthermore, both quantities in the integrand are odd functions of ω

[see Eqs. (3.2)—(3.4)], so the result vanishes. Thus the impurity does not affect the quantity

$$G_{\alpha\alpha}(0,0;\tau\to-0)=\frac{\rho_0}{2}\quad(\alpha=R,L)\ . \tag{3.9}$$

Turning to the anomalous Green's function, a straightforward calculation leads to the identity

$$G_{LR}^{(0)}(0,0;\tau\to-0)=[G_{RL}^{(0)}(0,0;\tau\to-0)]^*=-\frac{e^{i\varphi}\Delta_0}{2\pi v_F\hat{g}s}=-\frac{\rho_1}{2}e^{i\varphi}\ , \tag{3.10}$$

where Eqs. (3.5), (3.6), and (2.6) have been considered and the amplitude ρ_1 of the CDW has been introduced [see Eq. (2.13)]. The effect of the impurity on the anomalous Green's function is given by the following nontrivial integral,

$$G_{LR}(0,0;\tau\to-0)=-\frac{1}{2\pi v_F}\int_0^\infty d\omega\frac{\dfrac{e^{i\varphi}C(\omega)\Delta_0}{(\omega^2+\Delta_0^2)^{1/2}}+\dfrac{T}{2v_F}C^2(\omega)}{1+\dfrac{T}{v_F}\cos\varphi\dfrac{\Delta_0}{(\Delta_0^2+\omega^2)^{1/2}}C(\omega)+\left[\dfrac{T}{2v_F}\right]^2C^2(\omega)}\ , \tag{3.11}$$

which is obtained by inserting Eqs. (3.3), (3.4), (3.5), and (3.6) into Eq. (3.2).

In order to carry out analytical calculations, the integrand in Eq. (3.11) is approximated by choosing the following approximate form $C_{\rm app}(\omega)$ instead of the function $C(\omega)$ given by Eq. (3.6)

$$C_{\rm app}(\omega)=\begin{cases}1 & \text{for } \omega<\omega_0,\\ \dfrac{2}{\pi}\dfrac{D}{(\Delta_0^2+\omega^2)^{1/2}} & \text{for } \omega>\omega_0,\end{cases} \tag{3.12}$$

where $\omega_0=2D/\pi$, which reproduces $C(\omega)$ exactly in the limits of small and large ω. $C_{\rm app}(\omega)$ and $C(\omega)$ are depicted in Fig. 6 to give a good comparison.

The accuracy of this approximation will be checked in two different ways: (i) by calculating certain limit analytically; (ii) by numerical integration of the integral in Eq. (3.11).

Using the results derived above, different physical quantities will be calculated.

(i) Electron density at the impurity site. The electron density at $x=0$ given by Eq. (2.22) and it can be split into two parts arising from the normal and anomalous Green's functions as

$$\rho(0)=\rho_n(0)+\rho_a(0)\ , \tag{3.13}$$

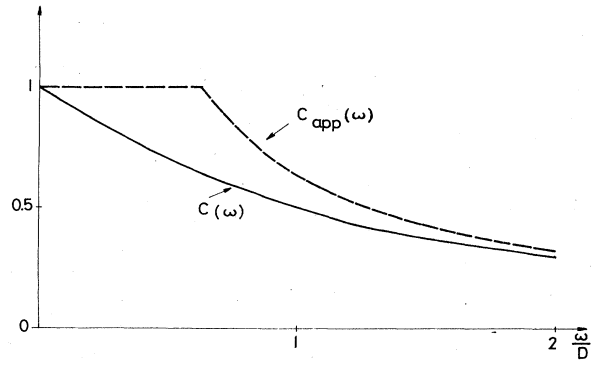

FIG. 6. $C(\omega)$ function (solid line) and its approximation $C_{\rm app}(\omega)$ (dashed line) given by Eq. (3.12).

where

$$\rho_n(0)=s\sum_{\alpha=L,R}G_{\alpha\alpha}(0,0,\tau\to-0)=s\rho_0\ , \tag{3.14}$$

and

$$\rho_a(0)=s[G_{LR}(0,0,\tau\to-0)+\text{c.c.}]\ , \tag{3.15}$$

where according to Eq. (3.9) the impurity affects only the anomalous part $\rho_a(0)$, which can be calculated by using Eq. (3.11). This is true only in the case of backward scattering because the forward scattering results in a contribution to $G_{\alpha\alpha}(0,0,\tau)$ which contains simultaneously parts even and odd in the energy.

The phenomenon of interest is that the impurity produces Friedel oscillations in the absence of the CDW, which hinders and modifies the formation of the Friedel oscillations. Thus, first $\rho_a(0)$ is calculated without the presence of the CDW. Using Eqs. (3.11), (3.15), and (3.6), one gets

$$\rho_a(0)=-\frac{2s}{\pi^2v_F}\int_0^\infty\frac{(T/\pi v_F)\arctan^2(D/\omega)}{1+(T/\pi v_F)^2\arctan^2(D/\omega)}d\omega\ , \tag{3.16}$$

which has been evaluated analytically in the limiting cases of small and large couplings. The results are

$$\rho_a(0)=-s\frac{T}{\pi v_F}\frac{4D}{v_F}\ln2\quad\text{for}\quad\left[\frac{T}{\pi v_F}\right]\ll1\ , \tag{3.17}$$

and

$$\rho_a(0)=-\text{sgn}(T)s\frac{D}{\pi v_F}=-\text{sgn}(T)s\rho_0\quad\text{for}\quad|T|\to\infty\ , \tag{3.18}$$

where in the second case only the large ω region contributes to the integral. The more accurate asymptotic form of $\rho_a(a)$ can be obtained by multiplying the right-hand side of Eq. (3.18) by $[1-(4v_F/\pi T)^2]$.

Thus, by considering Eqs. (3.13) and (3.18), one obtains in the infinitely strong-coupling impurity case

$$\rho(0)\to\begin{cases}0 & \text{for } T\to+\infty,\\ s\rho_0 & \text{for } T\to-\infty,\end{cases} \tag{3.19}$$

which means that the repulsive impurity pushes out all of the electrons and the attractive one fills up the band completely at the impurity site. The actual value of the latter result is sensitive to the form of the cutoff. The weak- and strong-coupling regions are separated by a crossover region of intermediate strength coupling $|T/2v_F|\sim 1$.

The case of mutual presence of the impurity and the CDW is more complicated. The integrand in Eq. (3.11) will be approximated by inserting $C_{\rm app}(\omega)$ instead of $C(\omega)$, and then the calculation of $\rho_a(0)$ becomes straightforward. The result is

$$\rho_a(0)=-\frac{\Delta_0}{\pi v_F}\cos\varphi\left[\frac{\arctan A}{A}+\frac{1-(T/2v_F)^2}{[1+(T/2v_F)^2]^2}B\right]-\frac{TD}{\pi^2 v_F^2}\left[\frac{\arctan A}{A}+\frac{1}{1+(T/2v_F)^2}\right] \tag{3.20}$$

where

$$A=\left[\left[\frac{\pi\Delta_0}{2D}\right]^2+\left[\frac{T}{2v_F}\right]\frac{\pi\Delta_0}{D}\cos\varphi+\left[\frac{T}{2v_F}\right]^2\right]^{1/2}, \tag{3.21}$$

$$B=\ln\frac{4D}{\pi\Delta_0}-\frac{t}{(1-t^2)^{1/2}}\arccos(t)\ , \tag{3.22}$$

with

$$T=\frac{(T/v_F)\cos\varphi}{1+(T/2v_F)^2}\ . \tag{3.23}$$

The validity of the approximation can be checked in the limits as $T\to 0$ and $T\to\pm\infty$.

As $T\to 0$ the present result can be compared with the exact result of Eq. (3.17). The relative error is $[\ln(2/\pi)+1]/\ln(2D\Delta_0^{-1})$ which is about 0.1 for $D/\Delta_0\sim 100$.

In the strong-pinning case, $T\to\pm\infty$, Eq. (3.20) provides

$$\rho_a(0)=-\rho_0\,\mathrm{sgn}(T)\left[1+O\left[\frac{1}{T^2}\right]\right]+\left[\cos\varphi\frac{4v_F}{T^2\pi}\Delta_0\ln\left[\frac{4D}{\pi\Delta_0}\right]+O\left[\frac{1}{T^3}\right]\right], \tag{3.24}$$

where the φ-independent and φ-dependent parts are calculated in different orders in $1/T$ as $T\to\pm\infty$. The terms given here can be reproduced exactly using the original form of the function $C(\omega)$.

The comparison of the approximation given by Eq. (3.20) with the numerical integration of the original integral in Eq. (3.11) shows that the error drops drastically as T increases. Namely at $T=0$ we have found an error of 10%, at $T/(2v_F)\sim 2$ the error is about 2%, and the result becomes exact as $T\to\pm\infty$.

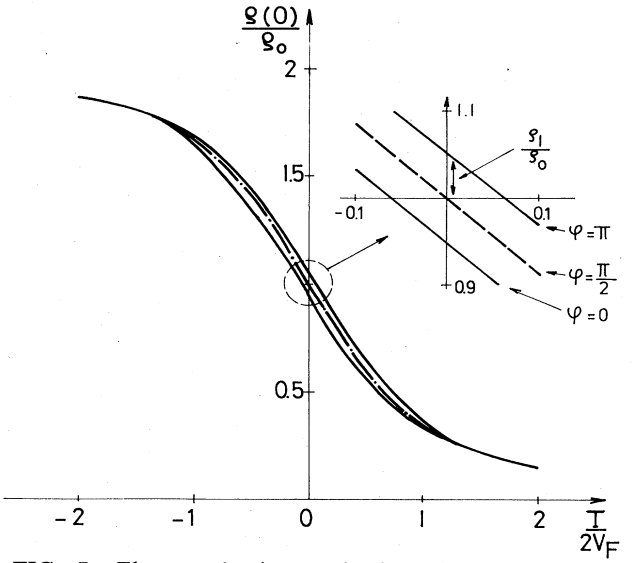

FIG. 7. Electron density at the impurity site is plotted against the dimensionless scattering strength for three different positions of the CDW. The details near zero coupling are enlarged.

The dependence of $\rho_a(0)$ on the dimensionless strength of the impurity coupling $T/2v_F$ is shown in Fig. 7 for three different CDW positions (values of φ). The findings can be summarized as follows.

In the *weak-coupling* limit [$|T/(2v_F)|\ll 1$], the CDW is slightly deformed, thus there are only small corrections to the cosine dependence of $\rho_a(0)$ on the CDW position [according to Eqs. (3.10) and (3.15), $\rho_a(0)=-\rho_1\cos(\varphi)$, see also Eq. (2.11)].

The *crossover* value of the *coupling* $T_{\rm cr}=\pm\pi v_F\Delta_0/\hat{g}D$ divides the two regions in which either the CDW or the effect of the impurities dominates the charge density $\rho(0)$ at the impurity site. Considering the realistic case $D/\Delta_0\gg 1$, the crossover coupling strength $T_{\rm cr}$ is in the weak-coupling region

$$\left|\frac{T_{\rm cr}}{2v_F}\right|\approx\frac{\pi}{2}\frac{1}{\hat{g}}\frac{\Delta}{D}\ll 1\ ,$$

as $\Delta_0/D\sim 10^{-2}$ and $\hat{g}\sim 0.1$.

The *intermediate-strength-coupling* region $|T/(2v_F)|\sim 1$ is dominated by the impurity effects at the impurity site $x=0$. In this region the dependence of $\rho_a(0)$ on the position of the CDW cannot be approximated by a simple $\cos\varphi$ [in this region, t as given by Eq. (3.23) is of the order of unity and this results in a complicated φ dependence of $\rho_a(0)$].

The *strong-coupling* region can be characterized by an almost completely occupied or empty electron band at the impurity site depending on the sign of the coupling [see Eq. (3.19)]. This behavior is influenced very slightly by the position of the CDW [see Eq. (3.24)]. In contrast to the intermediate-strength-coupling case, the φ dependence of $\rho(0)$ is again simply $\cos(\varphi)$-like.

(ii) $\delta\Omega$ thermodynamical potential due to the impurity.

As the force exerted by the impurity on the CDW will be calculated from $\partial\delta\Omega/\partial\varphi$, therefore, the main part of the discussion is left to Sec. V.

Using Eq. (2.25) for $\delta\Omega$ and the definition of $\rho_a(0)$ [Eq. (3.15)], the thermodynamic potential $\delta\Omega$ can be expressed in terms of $\rho_a(0)$ as

$$\delta\Omega(T)=s\int_0^T dT'\rho_a(0)\mid_{T'} . \tag{3.25}$$

The most striking feature of $\delta\Omega$ is that at large T,

$$\delta\Omega(T)=-s\mid T\mid\rho_0+O(T^0) , \tag{3.26}$$

which follows from Eq. (3.18).

A more accurate expression can be derived by using Eq. (3.11) and introducing $C_{\rm app}(\omega)$ instead of $C(\omega)$. The final result can be obtained using Eq. (3.20),

$$\delta\Omega=-\frac{4D}{\pi^2}\left[A\arctan A-\frac{\pi\Delta_0}{2D}\arctan\frac{\pi\Delta_0}{2D}\right]-\frac{\Delta_0}{\pi}\left[t\ln\left[\frac{4D}{\pi\Delta_0}\right]+(1-t^2)^{1/2}\arccos(t)-\frac{\pi}{2}\right] . \tag{3.27}$$

Concerning the accuracy of this expression, the discussion following the similar expression for $\rho_a(0)$ [Eq. (3.20)] holds.

It is interesting to note that in the large T limit the term depending on the position of the CDW is independent of T and that is proportional to $-\mathrm{sgn}(T)\Delta_0\cos\varphi$, which is a correction to the result given by Eq. (3.26).

(iii) Anomalous Green's function at the impurity site. The anomalous Green's function at $x=0$ is given by (3.11), where the time difference is $\tau\rightarrow-0$ as in the order parameter. In the absence of the impurity the anomalous Green's function $G_{LR}(0,0;\tau\rightarrow-0)$ describes the oscillating charge density in the CDW,

$$G_{LR}(0,0;\tau\rightarrow-0)=\frac{e^{i\varphi}}{sg}\Delta_0=-\frac{\rho_1}{2}e^{i\varphi} . \tag{3.28}$$

The main point of the present work is that the impurity induces the Friedel oscillations around the impurity which is described also by the anomalous Green's function. At small coupling, Eq. (3.11) has a simple form,

$$G_{LR}(0,0;\tau\rightarrow-0)=-\rho_1 e^{i\varphi}-\left[\frac{T}{2v_F}\right]\frac{2D}{\pi^2 v_F}\ln 2 , \tag{3.29}$$

and the CDW is only weakly perturbed.

In the case of infinitely strong coupling, the result

$$G_{LR}(0,0;\tau\rightarrow-0)=-\frac{D}{2\pi v_F}\mathrm{sgn}(T) \tag{3.30}$$

is not affected by the CDW, but is determined by the band cutoff D, which results in an upper limit for the oscillation amplitude just as in the case of the electron density $\rho(0)$ at the impurity site [see Eq. (3.19)].

For an arbitrary coupling strength T the ω-integral in the expression Eq. (3.11) can be approximated by introducing $C_{\rm app}(\omega)$, and the final expression is

$$\lim_{\tau\rightarrow-0}G_{LR}(0,0,\tau)=-\frac{\Delta_0}{2\pi v_F}e^{i\varphi}\left[\frac{\arctan A}{A}+\frac{B}{1+(T/2v_F)^2}\right]-\frac{TD}{2\pi^2 v_F^2}\left[\frac{\arctan A}{A}+\frac{1}{1+(T/2v_F)^2}\right]+\frac{2\Delta_0}{\pi v_F}\frac{B(T/2v_F)^2}{[1+(T/2v_F)^2]^2}\cos\varphi . \tag{3.31}$$

This expression reflects again the competition between the impurity and CDW, as in the expressions (3.20) and (3.27) for $\rho(0)$ and $\delta\Omega$.

The CDW order parameter modified by the impurity is defined as

$$\Delta(x)=-gsG_{LR}(x,x,\tau\rightarrow-0) . \tag{3.32}$$

Using Eq. (3.30), the rate of the enhancement of the order parameter at the impurity site can be obtained for infinitely strong coupling,

$$\frac{\Delta(0)}{\Delta_0}=s\frac{D}{\Delta_0}\mid\hat{g}\mid=s\frac{D}{\Delta_0}\frac{1}{1+\ln(4D/\pi\Delta_0)}(T\rightarrow+\infty) . \tag{3.33}$$

Thus the enhancement can be on the order of 20, as $D/\Delta_0\sim100$ and $\hat{g}\sim0.1$ for a typical CDW. The relative absolute value $\mid\Delta(0)/\Delta_0\mid$ for arbitrary coupling strength is calculated using Eqs. (3.31) and (3.32) and shown in Fig. 8 for three different positions of the CDW. In the competition between the CDW and the Friedel oscillations, the crossover occurs at the coupling strength $T_{\rm cr}$ defined in the discussion of $\rho(0)$. Depending on the relative position of the CDW and the impurity and on the sign of the coupling T, the interference between the CDW and Friedel oscillations may result in enhancement or in destruction. If the position of the CDW is such that the contribution of the Friedel oscillations and the CDW have the same amplitude but opposite signs a complete cancellation can occur, thus $\Delta(0)=0$. This can happen in the crossover-coupling region ($T\approx T_{\rm cr}$). As $\mid T_{\rm cr}\mid/(2v_F)\ll1$, in the intermediate-coupling region the Friedel oscillations always dominate. However, at the impurity site, $\mid\Delta(0)\mid/\Delta_0\gg1$ and the effect of the impurity drops off very fast inside the region of the CDW amplitude coherence length $\xi_0=v_F/\Delta_0$ (see Sec. IV). The phase Φ of the perturbed order parameter is also shown in Fig. 9 [$\Delta(0)=e^{i\Phi}\mid\Delta(0)\mid$].

IV. FRIEDEL OSCILLATIONS SUPERIMPOSED ON THE CDW

Until now, only the effect of the impurity at the impurity site has been studied. This section shows how the Friedel oscillations around the impurity are superimposed on the CDW.

For this problem we need the unperturbed Green's function $\hat{G}^{(0)}_{\alpha\beta}(x-x',i\omega_n)$ at finite space argument. Considering Eqs. (2.19), (2.20), and (2.21), the momentum integrals can be performed and one obtains (see Ref. 26)

$$\hat{G}^{(0)}_{RR}(x,i\omega_n)=\hat{G}^{(0)}_{LL}(-x,i\omega_n)=-\frac{i}{2v_F}\left[\frac{\omega_n}{(\omega_n^2+\Delta_0^2)^{1/2}}+\mathrm{sgn}(x)\right]\exp\left[-\frac{|x|}{v_F}(\Delta_0^2+\omega_n^2)^{1/2}\right], \tag{4.1}$$

and

$$\hat{G}^{(0)}_{LR}(x,i\omega_n)=\hat{G}^{(0)}_{RL}(x,i\omega_n)=-\frac{\Delta_0}{2v_F(\omega_n^2+\Delta_0^2)^{1/2}}\exp\left[-\frac{|x|}{v_F}(\Delta_0^2+\omega_n^2)^{1/2}\right]. \tag{4.2}$$

These expressions are valid in the range $|x|\gg v_F/D$. At the atomic and at smaller distances ($|x|\leq v_F/D$) the term proportional to $\mathrm{sgn}(x)$ in Eq. (4.1) decreases sharply and tends to zero as $x\to 0$. Furthermore, at small distances, for large energy ω_n, in addition to the decay factor $\exp[-|x|(\Delta_0^2+\omega_n^2)^{1/2}/v_F]$, another decay factor occurs in the expression for $\hat{G}^{(0)}_{\alpha\beta}(x,i\omega_n)$, which is similar to the function $C(\omega)$ introduced by Eq. (3.6). Due to the large symmetric momentum cutoff $p_0=D/v_F$ (see Fig. 4), in addition to the Friedel oscillations another type of rapid oscillatory term occurs. This term behaves as $\sin(p_0x)/p_0x$, which in contrast to the other terms at large distances $|x|>\xi_0$, does not contain the exponential decay factor $\exp[-|x|(\Delta_0^2+\omega_n)^{1/2}/v_F]$. This new term is a consequence of the sharpness of the momentum cutoff. Choosing a more realistic smooth cutoff, these new terms disappear. Thus, they are considered unphysical and will be dropped.

Using Eqs. (4.1) and (4.2) the Dyson equation (3.1) can be solved for $G_{\alpha\beta}(x,x,i\omega_n)$ in a straightforward manner, and the results are

$$G_{LR}(x,x,i\omega_n)=G^{(0)}_{LR}(0,i\omega_n)+\frac{T}{4v_F^2}e^{-iQx}\exp[-2|x|(\Delta_0^2+\omega_n^2)^{1/2}/v_F]$$

$$\times\frac{\Delta_0^2e^{2i\varphi}-2\omega_n^2-\Delta_0^2}{(\Delta_0^2+\omega_n^2)\left[1+\frac{T}{v_F}\cos\varphi\frac{\Delta_0C(\omega_n)}{(\Delta_0^2+\omega_n^2)^{1/2}}+\left[\frac{T}{2v_F}\right]^2C^2(\omega_n)\right]}, \tag{4.3}$$

and

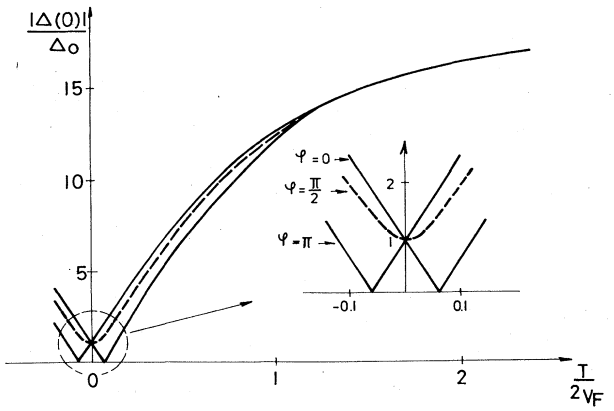

FIG. 8. Amplitude of the order parameter in Δ_0 units at the impurity site is plotted as the function of the dimensionless scattering strength for three different positions of the CDW. The details of the curves near zero coupling are enlarged.

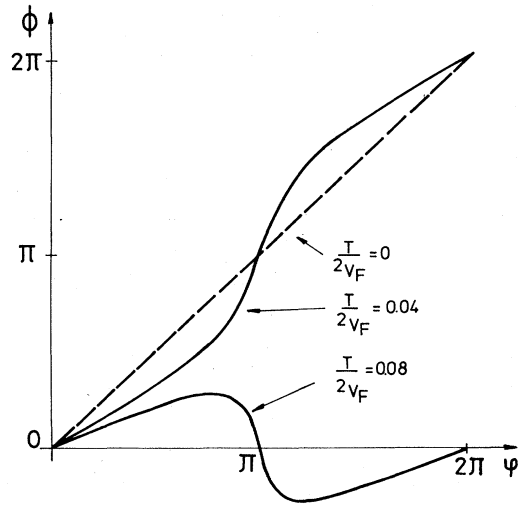

FIG. 9. The phase of the order parameter is plotted as the function of the CDW position for different values of the dimensionless scattering strength.

$$G_{LL}(x,x,i\omega_n)=G_{LL}^{(0)}(0,i\omega_n)-\frac{\Delta_0 T}{2v_F^2}\sin\varphi\exp[-2\,|\,x\,|\,(\Delta_0^2+\omega_n^2)^{1/2}/v_F]$$
$$\times\frac{1}{(\Delta_0^2+\omega_n^2)^{1/2}\left[1+\frac{T}{v_F}\cos\varphi\frac{\Delta_0 C(\omega)}{(\Delta_0^2+\omega_n)^{1/2}}+\left[\frac{T}{2v_F}\right]^2 C^2(\omega_n)\right]}\,. \tag{4.4}$$

Turning again to the zero temperature case, most of the integrals with respect to ω can be performed and one obtains for $|\,x\,|\gg v_F/D$

$$G_{LR}(x,x,\tau\to-0)=-\frac{\Delta_0}{2\pi v_F}e^{-iQx}\left\{\frac{1}{\hat{g}s}e^{i\varphi}+t_0\left[K_1\left[2\frac{x}{\xi_0}\right]-tK_0\left[2\frac{x}{\xi_0}\right]\right]\right.$$
$$\left.+\cos\varphi(t_0^2\cos\varphi-e^{i\varphi})\int_0^\infty\frac{\exp[-2x\cosh(y/\xi_0)]}{\cosh y+t}dy\right\}, \tag{4.5}$$

and

$$G_{LL}(x,x,\tau\to-0)=-\frac{\Delta_0}{2\pi v_F}\sin\varphi t_0\left[K_0\left[2\frac{x}{\xi_0}\right]-t\int_0^\infty\frac{\exp[-2x\cosh(y/\xi_0)]}{\cosh y+t}dy\right]. \tag{4.6}$$

where K_0 and K_1 are the modified Bessel functions and

$$t_0=t\,|_{\varphi=0}=\frac{T/v_F}{1+(T/2v_F)^2}\,, \tag{4.7}$$

and where t is given by Eq. (3.23). In the following we will use the expansions $K_0(x)\approx-\ln(x/2)$ and $K_1(x)\approx 1/x$ for $x\ll 1$, and the fact that the integral occurring in the expressions above is nonsingular as $x\to 0$.

The electron density can be obtained by inserting Eqs. (4.6) and (4.7) into Eq. (2.22), and one gets the following expression for the perturbation of the CDW

$$\rho(x)-\rho^{(0)}(x)=s\frac{t_0}{2\pi}\frac{\cos(Qx)}{|\,x\,|}\quad\text{for } v_F/D\ll|\,x\,|\ll\xi_0\,, \tag{4.8}$$

where only the most singular term in the variable x is kept, corresponding to the well-known Friedel oscillations around the impurity. It is interesting to note that according to Eq. (4.8) the charge density around the impurity $|\,x\,|\ll\xi_0$ is just the sum of the contributions corresponding to the CDW and to the Friedel oscillations. It can be seen from Eqs. (4.5) and (4.6) that there are further interference terms proportional to $t_0\Delta_0$, but they are less singular in x at small distances. For intermediate strength couplings at small distances, the Friedel oscillations dominate the CDW. Their amplitudes become comparable at a crossover distance $x_0=\xi_0 t_0\hat{g}s/2$. Beyond this distance, the CDW has the larger amplitude. Furthermore, at distances outside of the coherence length $|\,x\,|>\xi_0$, the Friedel oscillations cannot be formed, because, in the case of the free-electron gas, at such distances the Friedel oscillations that builds up of electron-hole pairs with energies smaller than the gap Δ_0, which are not available in the presence of the CDW. Thus the Friedel oscillations penetrate into the region $|\,x\,|>\xi_0$ by tunneling, which is manifested by the exponential decay of the modified Bessel functions for large arguments.

It is interesting to mention that the amplitude of the Friedel oscillations as a function of the coupling T has a maximum at $|\,T/2v_F\,|=1$ ($t_0=1$). Thus for larger coupling, it decreases. This is special for our model, where only the backward scattering is taken into account. In the present case, the effective coupling $t_0\to 0$ as $T\to\pm\infty$ in contrast to the more physical model with both forward and backward scattering where resonant scattering with phase shift $\pi/2$ corresponds to the infinitely strong coupling.

The CDW order parameter $\Delta(x)$ modified by the presence of an impurity can be obtained by inserting Eq. (4.5) into Eq. (3.32) and one obtains

$$\Delta(x)=\Delta_0 e^{-i(Qx-\varphi)}+s\frac{v_F}{2}\hat{g}t\frac{e^{-iQx}}{x}\,, \tag{4.9}$$

which is valid in the interval $v_F/D<|\,x\,|<\xi_0$. The function $\Delta(x)$ has a zero at $x=\pm x_0$ but only for special positions of the CDW, namely, at $\varphi=\pi$ for $T>0$ and at $\varphi=0$ for $T<0$.

V. DENSITY OF STATES AND BOUND STATES

The interaction of the electrons with the impurity modifies the electronic density of states. Furthermore, as has first been pointed out by Gor'kov and Dorokhov,[25] bound states may appear in the CDW gap localized around the impurity. Recently, Nozières[28] called the attention to the appearance of a bound pair of states above and below the conduction band.

A. Density of states

The electron density of states at position x is given by

$$\rho(x;\omega)=-\frac{1}{\pi}\lim_{i\omega_n\to\omega+i\delta}\mathrm{Im}(G_{RR}+G_{LL}+G_{RL}+G_{LR})_{x;i\omega_n}\,. \tag{5.1}$$

In the case of no impurity, the density of states is of the BCS type, and can be obtained by inserting Eqs. (3.4) and (3.5) into (5.1), and the result is

$$\rho^{(0)}(x;\omega)=\begin{cases}\dfrac{1}{\pi v_F}\dfrac{|\omega+\Delta_0\cos(Qx-\varphi)|}{(\omega^2-\Delta_0^2)^{1/2}} & \text{if } D\gg|\omega|>\Delta_0,\\ 0 \text{ if } |\omega|<\Delta_0,\end{cases} \tag{5.2}$$

where there is a $(\omega^2-\Delta_0^2)^{-1/2}$ singularity at the edge of the gap.

In the presence of the impurity, the density of states is obtained at the impurity site by considering Eqs. (3.2)—(3.5) and Eq. (5.1)

$$\rho(0;\omega)=\frac{1}{\pi v_F}\lim_{i\omega_n\to\omega+i\delta}\operatorname{Im}\left[\frac{C\left[\dfrac{\Delta_0\cos\varphi+i\omega_n}{(\Delta_0^2+\omega_n^2)^{1/2}}+\dfrac{TC}{2v_F}\right]}{1+\dfrac{T}{v_F}\dfrac{\Delta_0 C\cos\varphi}{(\omega_n^2+\Delta_0^2)^{1/2}}+\left[\dfrac{TC}{2v_F}\right]^2}\right]. \tag{5.3}$$

As we are interested in the region $|\omega|\ll D$, we may take $C(\omega)\approx 1$ [see Eq. (3.6)]. The final form obtained for $|\omega|>\Delta_0$ by analytical continuation is

$$\rho(0;\omega)=\frac{1}{\pi v_F}\frac{\left|\omega+\Delta_0\cos\varphi\dfrac{1-(T/2v_F)^2}{1+(T/2v_F)^2}\right|}{\left[1+\left[\dfrac{T}{2v_F}\right]^2\right](\omega^2-\Delta_0^2)^{1/2}\left[1+\left[\dfrac{\Delta_0 t}{(\omega^2-\Delta_0^2)^{1/2}}\right]^2\right]}. \tag{5.4}$$

The main new feature of this result is that the density of states is rounded in the region $|\omega|\gtrsim\Delta_0$, as $\rho(0;\omega)\sim(\omega^2-\Delta_0^2)^{1/2}$. At the points $\omega=\pm\Delta_0$ of the previous singularities $\rho(0;|\omega|=\Delta_0)$ becomes zero (see Fig. 10). This formula shows also that in the case of no CDW the density of states near the Fermi level $|\omega|\ll D$ is always suppressed by the impurity as $\rho(0,\omega)\sim[1+(T/2v_F)^2]^{-1}$. That is a consequence of the formation of the bound state outside the conduction band, which will be discussed at the end of this section.

B. Bound states in the gap

Using Eq. (5.3), the density of states in the gap is obtained by analytical continuation,

$$\rho(0;\omega)=\begin{cases}Z_\pm\delta(\omega\mp\omega_0) & \text{if } T\cos\varphi<0,\\ 0 \text{ if } T\cos\varphi>0,\end{cases} \tag{5.5}$$

for $|\omega|<\Delta_0$, where the energy of the bound state ω_0 is

$$\omega_0=\Delta_0(1-t^2)^{1/2} \tag{5.6}$$

and the strength of the pole is

$$Z_\pm=2\frac{\Delta_0}{v_F}\frac{|t|}{1+(T/2v_F)^2}\left[\frac{1}{2}\pm\frac{[1-(T/2v_F)^2]\cos\varphi}{2\{[1-(T/2v_F)^2]^2+[(T/v_F)\sin\varphi]^2\}^{1/2}}\right]. \tag{5.7}$$

The pair of bound states is obtained only if the perturbation of the electron gas by the impurity is out of phase with the unperturbed CDW ($T\cos\varphi<0$). The positions of these bound states are symmetric with respect to the Fermi level, but their weights are different. For weak coupling $|T/2v_F|\ll 1$, the binding energy goes as $\omega_0\sim t^{-2}$ and $Z_\pm\sim t$. In the special case $t=-1$ the two bound states collapse and they are at the Fermi level $\omega_0=0$. For even stronger coupling, the energy of the bound state ω_0 goes to the continuum again which might be a special consequence of the backscattering. The expression in the large parentheses on the right-hand side of Eq. (5.7) is always less than unity, thus

$$Z_\pm<2\frac{|t|}{1+(T/2v_F)^2}\frac{1}{\xi_0}, \tag{5.8}$$

where the BCS length is introduced.

The extension of the wave function of the bound state in the real space is estimated by studying the density of states in the gap far from the impurity using Eqs. (4.3) and (4.4). The dependence on x arises from the exponential factor, which after analytical continuation has the form

$$\exp[-2|x|(\Delta^2-\omega_0^2)^{1/2}/v_F]=\exp(-2|x||t|/\xi_0),$$

where t is given by Eq. (3.23), and ξ_0 is introduced and Eq. (5.6) is taken into account. Thus the size of the bound-state wave function is $r_0=\xi_0/|t|$, which is larger than the BCS length ξ_0 as $|t|<1$. This result is coherent with the weight factor $Z_\pm$ of the bound state at $x=0$, as the amplitude of the wave function at $x=0$ is inversely proportional to the size of the state [compare with Eq. (5.8)].

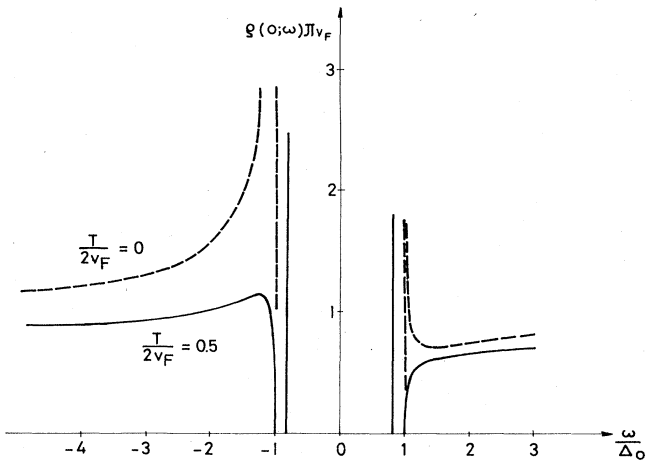

FIG. 10. Energy dependence of the density of states at the impurity site at $\varphi=3\pi/4$ for a typical value of the impurity-scattering strength $T/2v_F=0.5$ (solid line). A pair of bound states is indicated by the vertical lines at energies $\omega_0=\pm 0.82\Delta_0$. Without impurity, the dashed line shows the BCS-type singularity at energies $\omega=\pm\Delta_0$.

C. Bound state outside the conduction band

Nozières[28] pointed out the existence of a pair of bound states which occur for arbitrary values of the coupling strength. For weak coupling these bound states are just near the conduction band, and therefore their behavior is sensitive to the band and the cutoff chosen. The more striking limit is the strong-coupling case, where our result must be independent of the detailed features of the model, because the binding energy can be large compared with the bandwidth. The energy of the bound state $\bar{\omega}_0$ is determined from Eq. (5.3) at the point $x=0$, and using either the approximation $C(\omega_n)\sim(2/\pi)(D/\omega_n)$ or $C(\omega)=i(2/\pi)(D/\omega)$ [see Eq. (3.6)]. There are two bound states with energy $\pm\bar{\omega}_0$, where

$$\bar{\omega}_0=\left|\frac{T}{v_F}\right|\frac{1}{\pi}D\ . \tag{5.9}$$

In the case $T\to-\infty$ ($T\to\infty$) the density of states outside the conduction band is large only below (above) the Fermi level; thus, e.g., for $T/(2v_F)\ll-1$,

$$\rho(0;\omega<(-D))=\frac{D}{\pi v_F}\delta(\omega+|TD/\pi v_F|)\ .$$

Furthermore, according to Eq. (5.4) the density of states in the conduction band disappears in the large-T limit ($T\to\pm\infty$). Thus, in the limit $T\to\infty$ ($T\to-\infty$) at the impurity site, all of the density is concentrated in the very high- (low-) lying bound state, which is unoccupied (occupied) and gives the total electron density at the impurity site given by Eq. (3.19). In this consideration, the correct analytical continuation of $(\Delta_0^2+\omega_n^2)^{1/2}$ is important when Eq. (5.3) is evaluated. It can be shown that these bound states are mainly localized on the impurity site [see Eqs. (4.3) and (4.4)]. Finally, the interaction energy $\delta\Omega$ given by Eq. (3.26) is exactly the energy of the bound state $\bar{\omega}_0$, which can be seen by comparing Eq. (5.9) with Eq. (2.12).

VI. PINNING FORCE

The interaction between the CDW and the impurities results in a force acting on the CDW. The force depends on the positions of the impurities relative to the CDW. As far as the CDW position can be characterized by only a single phase φ, the force depends on the quantities $QR_i-\varphi=\varphi_i-\varphi$, where i labels the impurity with position R_i and $\varphi_i=QR_i$. The position of the CDW can be characterized by a single phase φ only if the size of the CDW considered is smaller than the Lee and Rice[9] phase coherence length $\xi_{\rm ph}$, which is much larger than the BCS amplitude-coherence length (in the case of the weak pinning $\xi_{\rm ph}\gg\xi_0$ as $\xi_{\rm ph}>10^{-4}$ cm and $\xi_0\geq 10^{-6}$ cm), but they are comparable in the case of strong pinning. As we have seen in the previous section, each impurity deforms the CDW well inside the range of the length ξ_0. If the distances between the impurities are smaller than ξ_0, then the forces exerted by the impurities are not additive, because the Friedel oscillation-type deformations overlap, and interference terms appear in the energy. In this case clusters of impurities must be considered. In order to avoid these difficulties, only a single impurity will be considered. If the CDW were completely rigid, then the force would be proportional to $\sin(\varphi_i-\varphi)$.[5,8] In the real case, however, the CDW is deformed around the impurity. Therefore, the simple sinusoidal dependence might be strongly modified. For the sake of simplicity, the impurity is considered with position $X=0$, thus $\varphi_i=0$.

The pinning force can be defined in two different ways.

(i) Thermodynamical perturbation theory has been used in Sec. III to calculate the interaction energy $\Omega(\varphi)$ between the CDW and the impurity [see Eq. (3.27)]. The force can be defined as the derivative of this energy $\Omega(\varphi)$ with respect to the position of the CDW, thus

$$F_{\rm th}=-Q\frac{\partial\Omega}{\partial\varphi}\ , \tag{6.1}$$

where Q is the proportionality factor between the position and the phase.

(ii) By using time-dependent perturbation theory based on adiabatic switching the force can be defined as the rate of the change of the momentum P carried by the electrons due to the impurity

$$F_{\rm ad}=\left\langle\frac{\partial P}{\partial t}\right\rangle\ , \tag{6.2}$$

where the total momentum P of the electrons is

$$P=\sum_k k a_k^\dagger a_k\ . \tag{6.3}$$

This expression can be simplified essentially by assuming that the electron gas is perturbed only in the vicinity of the Fermi energy. Thus, in this case,

$$P_{\rm app}=\frac{Q}{2}(N_R-N_L) \tag{6.4}$$

is a very good approximation for P and is widely used in the case of a one-dimensional electron gas.

In this section we consider the first definition and in Appendix B show the equivalence of the two definitions discussed above, where complete agreement has been found by calculating the second and third orders in perturbation theory. This complete equivalence, however, is somewhat surprising, as $P_{\rm app}$ rather than the exact definition (6.3) but has been used for the total momentum P. In order to clarify this point, we also show that for the thermal average of $\partial P_{\rm app}/\partial t$, the identity

$$\left\langle \frac{\partial P_{\rm app}}{\partial t} \right\rangle_{\rm th} = -Q\frac{\partial \Omega}{\partial \varphi} \tag{6.5}$$

holds to all orders in perturbation theory. This result strongly indicates that in the backscattering model, the application of the approximate form $P_{\rm app}$ leads to exact results.

In the following, after proving the identity (6.5), the actual expression of the force is calculated by using the first definition.

The operator $\partial P_{\rm app}/\partial t$ is calculated by using the Hamiltonian (2.16), and one obtains

$$\frac{\partial P_{\rm app}}{\partial t} = -i(PH) = QT[\psi_R^\dagger(0)\psi_L(0) - \psi_L^\dagger(0)\psi_R(0)] , \tag{6.6}$$

which is similar to the accelerator operator introduced by Barnes and Zawadowski.[13] The thermal average of this expression can be given in terms of the anomalous Green's function (see Sec. III) and the result is

$$\left\langle \frac{P_{\rm app}}{\partial t} \right\rangle_{\rm th} = iQs[G_{LR}(0,0,\tau\to -0) - G_{RL}(0,0,\tau\to -0)] , \tag{6.7}$$

where the spin degeneracy is also taken into account. On the other hand, $\partial\Omega/\partial\varphi$ can be calculated on the basis of Eq. (2.25) of Ω. Inserting the expressions (3.2) and (3.3) the integral with respect to T' can be performed exactly in Eq. (2.25), which yields the right-hand side of Eq. (6.7). Thus (6.5) holds.

The pinning force $F_{\rm th}$ given by Eq. (6.1) can be calculated by using the expression (3.11) for Ω, and one obtains

$$F_{\rm th} = -Q\frac{\partial\Omega}{\partial\varphi} = -sQ\frac{T}{\pi v_F}\sin\varphi \int_0^\infty d\omega \frac{C(\omega)\Delta_0(\Delta_0^2+\omega^2)^{-1/2}}{1+(T/v_F)\cos\varphi C(\omega)\Delta_0(\Delta_0^2+\omega^2)^{-1/2}+(T/2v_F)^2C^2(\omega)} , \tag{6.8}$$

where the function $C(\omega)$ is defined by Eq. (3.6). The integral with respect to ω can be carried out in the weak- and the strong-coupling limits, and the results are

$$F_{\rm th} = \begin{cases} -Q\dfrac{\Delta_0}{\pi}\dfrac{T}{v_F\hat{g}}\sin\varphi & \text{if } \left|\dfrac{T}{2v_F}\right| \ll 1 , \qquad (6.9) \\ Qs\Delta_0\sin\varphi\,\mathrm{sgn}(T) & \text{if } \left|\dfrac{T}{2v_F}\right| \gg 1 . \qquad (6.10) \end{cases}$$

In both cases, the pinning force shows a sinusoidal $\sin\varphi$ dependence on the position φ of the CDW. This form is strongly modified in the intermediate strength coupling region. In order to show that, the function $C(\omega)$ is approximated by $C_{\rm app}(\omega)$ as given by Eq. (3.12), and the integral can be performed. The result is

$$F_{\rm th} = -Qs\Delta_0\frac{T}{\pi v_F}\sin\varphi \left[\frac{\ln\left[\dfrac{4D}{\pi\Delta_0}\right] - \dfrac{t}{(1-t^2)^{1/2}}\arccos(t)}{1+\left[\dfrac{T}{2v_F}\right]^2} + \frac{\arctan A}{A} \right] , \tag{6.11}$$

where the notations are introduced in Sec. III and the error due to the approximation in $C(\omega)$ has also been discussed there. The dependence of the force on the coupling strength T is shown for three different values of φ in Fig. 11. The dependence on φ is clearly not sinusoidal, as the force for $\varphi=\pi/6$ is different for φ and $\pi-\varphi$ as is shown in Fig. 11. The deviation from the sinusoidal form is the largest around the coupling strength $|T/2v_F| \sim 1$, where the amplitude of the force shows a maximum. The position dependence of the force is shown in Fig. 12 for an intermediate coupling $T/2v_F \sim 0.9$.

The origin of the large deviation from the sinusoidal form can be traced back by noticing that the denominator of the integrand in Eq. (6.8) has a zero at $\omega=0$ for the parameter values $T/2v_F=1$ ($T/2v_F=-1$), $\varphi=\pi$ ($\varphi=0$) and the integral becomes divergent. In the region around these parameter values the integral is anomalously large.

Finally, we comment on the position dependence of the force $F_{\rm th}(\varphi)$ and the potential $\Omega(\varphi)$. In the intermediate-strength-coupling region $T/2v_F \sim 1$, the force is linear around the stable equilibrium position $\varphi=0$ of the CDW. The interval in which the force is linear (see Fig. 12) or the potential is quadratic (see Fig. 13) is larger than in the case of a sinusoidal potential. Thus the renormalized potential has a stronger resemblance to a periodic quadratic potential than to the sinusoidal potential. Furthermore, the top region at the maximum is narrower. For negative coupling $T/2v_F \sim -1$, the stable equilibrium position is at $\varphi=\pm\pi$, but the main features are unchanged.

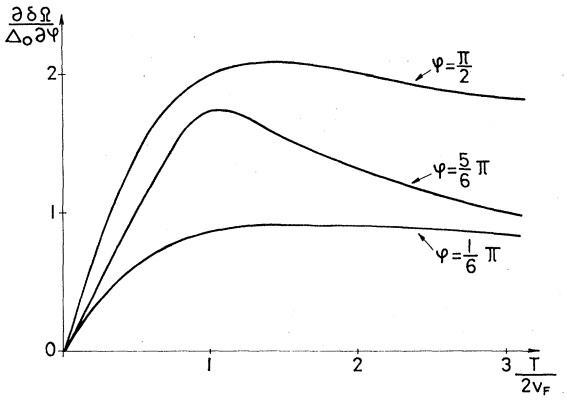

FIG. 11. Dependence of the force on the dimensionless impurity-scattering strength at three different positions of the CDW. The difference between the curves for $\varphi=\pi/6$ and $\varphi=5\pi/6$ demonstrates the anharmonic feature of the thermodynamical potential.

VII. CLASSICAL EQUATION OF MOTION WITH A DEFORMABLE CDW

In this section we generalize the classical model for the motion of the CDW. In the original model, the CDW was treated as a classical object and its position was characterized by a single coordinate $x=Q^{-1}\varphi$. This object was moving in a periodic potential with periodicity $\lambda=2\pi Q^{-1}$, which was representing the interaction between the CDW and the impurities. As the phase of the CDW can be deformed, however, only a domain of size of the phase coherence length $\xi_{\rm ph}$ can be described by the classical model. In this case the potential arises from the impurities in such a domain. If the number of the impurities in the domain is very large, there is a large destructive interference among the forces exerted by the impurities, as a homogeneous average over the impurity positions leads to complete cancellation. Thus, only the fluctuations in the impurity positions are responsible for a finite force. The position of the potential in real space is determined by the phase $\varphi_i=QR_i$ of those impurities, which corresponds to the largest fluctuation in the distribution of the impurity phases φ_i. The resulting force is similar to one due to a single impurity, but the amplitude is proportional to the amplitude of the fluctuations in the impurity phases, thus it is proportional to $N_{\rm imp}^{1/2}$, where $N_{\rm imp}$ is the number of impurities in a domain. In the original classical model the periodic potential was either sinusoidal or parabolic. In the present case according to the discussion at the end of Sec. VI and Fig. 13, the shape of the potential is strongly perturbed by the interaction, and it is between a sinusoidal and and quadratic one.

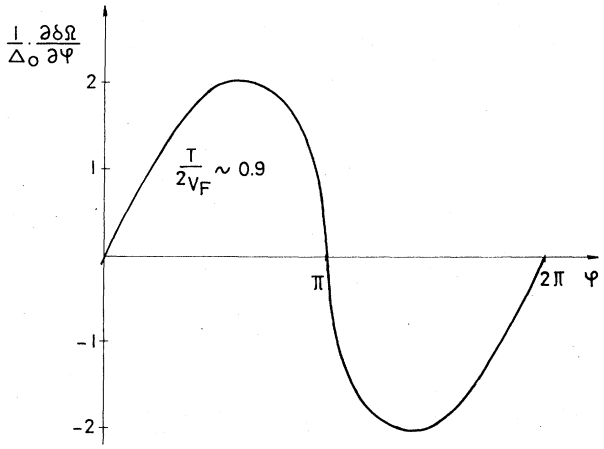

FIG. 12. The dependence of the force as the function of the CDW position at a typical value of the coupling strength $T/2v_F=0.9$.

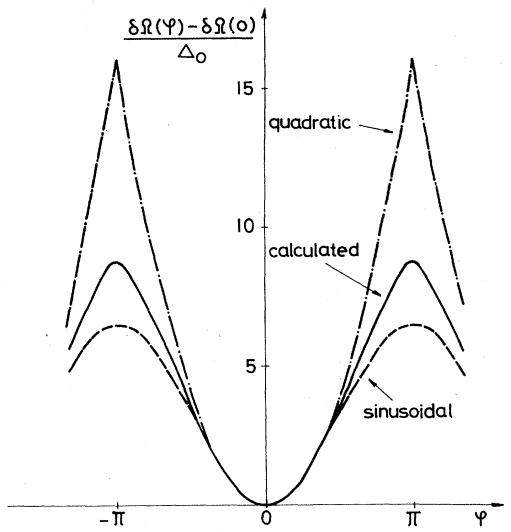

FIG. 13. Effective potential (solid line) acting on the CDW is plotted as the function of the CDW position at a typical value of the coupling strength $T/2v_F=0.9$. For comparison a quadratic (dotted-dashed line) and a sinusoidal (dashed line) potential fitted to the effective potential at $\varphi=0$ are also shown.

The classical equation of motion for a domain can be written as[5,6]

$$m^*\frac{d^2x}{dt^2}+\gamma\frac{dx}{dt}=-eNE+F\ , \tag{7.1}$$

where m^* is related to the Fröhlich mass, x is the coordinate $x=\varphi/Q$, γ is the damping, E is the electric field, N is the number of electrons in the domain, and F is proportional to the force calculated in Sec. VI, thus $F=-\alpha Q(\partial\Omega/\partial\varphi)$, where α is a proportionality factor depending on the impurity distribution, etc. Assuming that the motion of the CDW is overdamped the inertia term is dropped in most of the works. In this case the equation of motion for the phase is

$$\frac{d\varphi}{dt}=\dot{\varphi}=-\frac{Q}{\gamma}NeE-\frac{1}{\gamma}\alpha Q^2\frac{\partial\delta\Omega(\varphi)}{\partial\varphi}\ . \tag{7.2}$$

In the weak- and strong-coupling cases, the force is sinusoidal in a fairly good approximation [see Eqs. (6.9) and (6.10)], thus

$$F=-\alpha Q\Delta_0\delta\sin\varphi\ , \tag{7.3}$$

where δ is the following parameter:

$$\delta=\begin{cases}\dfrac{T}{\pi v_F\hat{g}} & \text{if } \dfrac{|T|}{2v_F}\ll 1,\\ \mathrm{sgn}(T)s & \text{if } \dfrac{|T|}{2v_F}\gg 1,\end{cases} \tag{7.4}$$

and for the sake of brevity, the equilibrium position determined by the impurity distribution is taken to be at $\varphi=0$.

The solution of Eq. (7.2) with the force (7.3) is

$$\frac{d\varphi}{dt}=-\frac{eNQ}{\gamma}\frac{E^2-E_T^2}{E-E_T\cos(\omega_0 t)} \quad \text{if } E>E_T\ , \tag{7.5}$$

where

$$E_T=\Delta_0\frac{Q\alpha}{eN}\,|\,\delta\,| \tag{7.6}$$

is the threshold field above which periodic motion exists and the frequency ω_0 corresponds to the periodicity of the motion of the classical object,

$$\omega_0=\frac{QeN}{\gamma}E_T\left[\left[\frac{E}{E_T}\right]^2-1\right]^{1/2}. \tag{7.7}$$

As it has been shown previously,[5,6,29] the motion in the periodic potential becomes very strongly anharmonic as the electric field approaches the threshold field E_T. The Fourier expansion of the solution of Eq. (7.3) is[28]

$$\frac{dx}{dt}=I_0+\sum_{n=1}^{\infty}I_n\cos(n\omega_0 t) \tag{7.8}$$

where

$$I_n=-\frac{en}{\gamma}(E^2-E_T^2)^{1/2}\left\{\frac{E}{E_T}-\left[\left[\frac{E}{E_T}\right]^2-1\right]^{1/2}\right\}^n. \tag{7.9}$$

The ratio of the subsequent harmonics I_{n+1}/I_n is a measurable quantity and the present model gives

$$\frac{I_{n+1}}{I_n}=\frac{E}{E_T}-\left[\left[\frac{E}{E_T}\right]^2-1\right]^{1/2} \tag{7.10}$$

for the weak- and strong-coupling limits.

Considering the intermediate-strength-coupling region around $T/2v_F\sim 1$, the equation of motion (7.2) cannot be solved by analytical methods. Using the numerical solution of that equation the Fourier coefficients can be determined numerically. The ratios of the subsequent harmonics are shown as a function of n for different CDW current in Fig. 14. It turns out that the character of the solutions in the intermediate-strength-coupling region $T/2v_F\sim 1$ is not very different from the weak- and strong-coupling results, in spite of the strong anharmonicity characterizing the pinning force. The only significant difference is in the frequency spectra of the ratios of the subsequent harmonics, which is no longer independent of n, as is indicated by Eq. (7.10), and they are enhanced at larger electronic fields. This enhancement does not mean, however, that the intensity of higher harmonics could exceed the intensity of the first one. The temperature dependence of these ratios will be shortly discussed in the Conclusion.

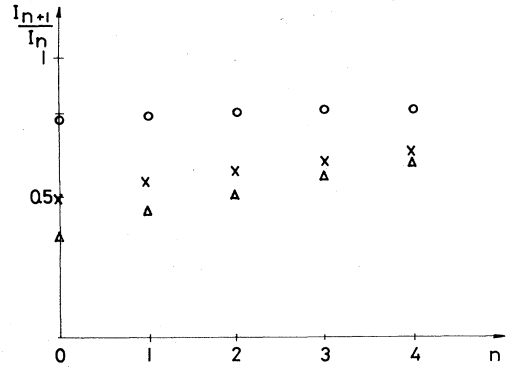

FIG. 14. Ratio of the intensity of the subsequent harmonics in the narrow band noise I_{n+1}/I_n is plotted as the function of n for different values of the CDW current i_0 (circles), $3i_0$ (crosses), and $5i_0$ (triangles), where i_0 is an arbitrarily chosen current flow using an electric field just above the threshold field E_T. The value of the dimensionless coupling strength is $T/2v_F=0.8$.

VIII. CONCLUSION

Bardeen[11] has pointed out that quantum phenomena might play an important role in the dynamics of sliding CDW. The subject of the present paper is the quantum corrections to the distortion of the CDW around a single impurity, thus all the terms of the perturbation series in the backward scattering by an impurity are summed up. The results obtained have been interpreted as a competition between the CDW and the Friedel oscillations formed around an impurity. These calculations are the extension to all orders in the perturbation series of the previous results derived by Barnes and Zawadowski,[13] using the analogy with the Josephson junction. The results presented here reproduce those obtained previously in second order perturbation theory.

The scheme of the present paper is that the interaction leading to the formation of the CDW is treated in the mean-field approximation, which is at first taken as in the absence of the impurity. This approximation is checked in Appendix C. There it is shown that the renormalization of the mean field by the impurity is equivalent to the adjustment of the impurity potential by approximately 10%. Thus the qualitative features of the present results are not altered.

The method applied is the equilibrium thermodynamic Green's function technique. For comparison the time-dependent perturbation theory is also used, with adiabatic switching of the impurity potential as has been done in the previous work.[13] The equivalence of these two methods is checked in the first three orders of perturbation theory.

In the model treated here, the electrons are strictly one dimensional and have linear dispersions. The latter restriction does not affect the results essentially. Further-

more, in the impurity scattering, only the backward scattering is kept. In a realistic case the forward scattering is also important. The role of the forward scattering is under study and that will be presented elsewhere.[30]

The calculations are performed at zero temperature to keep the calculations as simple as possible. The previous calculation based on the singularity to the Josephson junction has been carried out, for arbitrary temperature however.[13] The CDW acceleration due to the impurity obtained previously goes to zero faster than the CDW energy gap in second order in the perturbation. These results indicate that all of the higher-order corrections tend to zero faster than the first order classical term as the temperature approaches the CDW critical temperature T_c. Thus, in the vicinity of T_c, the classical theory is correct. It is worthwhile to mention the well-known result that the size of the Lee-Rice domain inside which the phase of the CDW is coherent, becomes infinitely large as the critical temperature is approached.

The one-dimensional (1D) nature of the model treated here does not affect most of our results as far as the phase of the CDW is slowly varying outside the region of the Friedel oscillations. Considering, e.g., the charge density at the impurity site, the Green's function $G(0,0;i\omega_n)$ with space coordinates taken at the impurity site occurs, which is not very sensitive to the 1D nature. The Friedel oscillations and, especially, their extension in the perpendicular direction are very sensitive to the three-dimensional (3D) character. The region where the Friedel oscillations dominate the CDW has a cigar shape. The situation is, however, completely different in the case of a very strong impurity. In the strictly 1D case, the impurity divides the CDW into two parts and the phases of these parts are arbitrary on the two sides of the impurity. The electron can pass the impurity only by tunneling. Furthermore, the tunneling of an electron-hole pair through the barrier couples the two CDW's on different sides and there is a coupling energy similar to the case of Josephson junctions. The situation is very different in 3D, because a single impurity cannot divide the CDW into two pieces, thus that can only distort the CDW strongly around the impurity.

All of our results are expressed in terms of the dimensionless backscattering strength $T/2v_F$. Taking a square-like potential barrier with height V and thickness d (atomic distance $< d < \xi_0$) the order of magnitude of the backscattering amplitude can be estimated as $T \sim Vd$, thus $T/2v_F \sim \hbar^{-1} Vd/v_F \sim V/D$. Thus the weak- and strong-coupling terminologies are very close to those used by Lee and Rice.[8]

Our results concerning the Friedel oscillations superimposed on the CDW can be summarized as follows.

(1) If $|T/2v_F| \ll 1$, the CDW is only weakly perturbed.

(2) If $|T/2v_F| \lesssim 10^{-1}$, the Friedel oscillations have a larger amplitude at the impurity site than the amplitude of the CDW. Furthermore, the phase of the oscillations around the impurity is locked to the impurity.

(3) If $|T/2v_F| \sim 1$, the Friedel oscillations even affect states at the band edges.

(4) If $|T/2v_F| \gg 1$, the top of the Friedel oscillations is chopped off at the band cutoff.

In the realistic cases $|T/2v_F|$ is not extremely weak; nor is it likely to be larger than unity. Thus, $|T/2v_F| \sim 0.1-1$.

The effect of the impurity on the density of states at the impurity site is to destroy the singularity at the edge of the gap, making it smoothly rounded as is shown in Sec. V. If the Friedel oscillations are out of phase relative to the CDW, then a pair of bound states occurs in the gap. In the strong-impurity case, the CDW is strongly deformed[8] and the Friedel oscillations are never out of phase. Thus the bound states are not formed. In the case of weak impurities, the relative impurity phase $\varphi_i = QR_i - \varphi$ is a random variable and the energies of the bound states depend on the position of the impurity relative to the CDW. Considering the density of states at the impurity sites if the average is taken over the impurity phase φ_i, then one finds that some parts of the gap near to the gap edges are filled with states. As the extension of the bound states in real space is at least the amplitude coherence length ξ_0, we predict that the gap edges are smeared out if the averaged impurity distance is comparable to or smaller than the coherence length ξ_0. That must be seen in the optical or tunneling experiments.[30] The bound states happen to be very similar to the two proton bound states with zero total momentum in superfluid He_4.[31]

Outside the conduction band another pair of the bound states always occurs for arbitrary coupling T. If the coupling is weak $|T/2v_F| \ll 1$, then these states are sensitive to the details of the band structure near to the energy cutoff. In contrast to the bound states in the gap, these bound states are well localized around the impurity site as their binding energy is large. The existence of these bound states is independent of the details, however, e.g., the bound states exist for a tight-binding band with even larger binding energy.[30]

The Friedel oscillations are formed well above the CDW transition temperature. The occurrence of the gap below T_c appears as a cutoff in the long-distance tail of the Friedel oscillations at distances greater than the amplitude coherence length ξ_0. As the gap increases, the Friedel oscillations become more localized in real space. Furthermore, it is shown [see Eq. (4.8)] that to a good approximation, inside the amplitude coherence length, the Friedel oscillations and the CDW are only superimposed. The crossover distance x_0, where the Friedel oscillations and the CDW have comparable amplitudes, is approximately $x_0 \lesssim 10^{-1}\xi_0$ for a realistic case.

The NMR and x-ray scattering are the appropriate tools to study the Friedel oscillations. In principle, the Friedel oscillations appear as a short-range order in the x-ray diffraction pattern. In the case of magnetic impurities,[21] these oscillations are momentarily magnetically polarized. Thus they must show up in the magnetic form factor of the impurity, which can be studied by incoherent neutron scattering.

The force exerted by the impurity is calculated as the derivative of the interaction energy with respect to the CDW position [see Eq. (6.1)]. On the other hand, Barnes and Zawadowski have calculated the acceleration of the CDW using a time-dependent technique.[13] The results

obtained by these two different techniques are compared in Sec. VI and Appendix B, and through the first three orders of perturbation theory, complete agreement is found. Concerning the force F, the main result is that it depends on the CDW position approximately in a sinusoidal form, and strong deviation from that occurs only in the range $|T/2v_F| \sim 1$.

The deviation from the sinusoidal form of the force has observable consequences when dc and ac voltages $[V = V_0 + V_1 \sin(\omega t)]$ are applied simultaneously to the sample. Varying the dc voltage V_0 causes the frequency $\omega_0(V_0)$ of the generated narrow band noise changes also. At the voltages V_0 for which the ratio of the generated narrow-band noise frequencies to the frequencies ω of the applied ac voltage is a rational number, so called Shapiro steps[7,32,33] occur in the dc current as a function of the dc voltage V_0. Theoretically, if the equation of motion given by Eq. (7.2) is overdamped and the force is sinusoidal, then the Shapiro steps occur only at harmonics and not at subharmonics.[34] As is shown in Sec. VI the force is never exactly sinusoidal. Therefore, the subharmonics must appear, in agreement with the experiments.[32,35,36]

Concerning the generated narrow-band noise discussed in Sec. VII our results and their consequences can be summarized as follows.

The first harmonic with the so-called washboard frequency ω_0, predicted by the classical theory, must always be present.

There are contributions to the harmonics of higher order due to the anharmonicity of the effective potential derived in Sec. VI.

Approaching the critical temperature of the CDW the contributions to the harmonics of higher order arising from the anharmonicity of the effective potential gradually disappear and near to the transition temperature the model with the sinusoidal potential becomes more accurate. In this case, the ratios of the intensities of the harmonics are given by Eq. (7.10).

In the case of backscattering and single impurities in the range of the BCS coherence length, the intensities of the harmonics are gradually decreasing with increasing n $(I_n > I_{n+1})$.

The case with several impurities inside the BCS coherence length is not considered, but it is very likely that it does not change the main behavior described above.

The forward scattering however, plays, an important role, and preliminary studies shows that the effective potential may be further modified and in some special cases the second harmonic might be larger than the first.[30]

Magnetic impurities due to the exchange coupling with the conduction electrons contribute to the intensity of higher harmonics, but not to the first one.[21]

There has been some speculation concerning experimental data that the lowest observable harmonics might have the frequency twice the washboard frequency $\omega = 2\omega_0$.[19] This speculation is not supported by the present study. In the case of $(TaSe_4)_2I$, however, the intensity of the second harmonic I_2 exceeds the intensity of the first I_1 at low temperature. Furthermore, as the critical temperature is approached, the intensity of the second harmonic I_2 decreases faster than that of the first I_1, and the first becomes the largest.[37] This behavior is consistent with the assumption that the large second harmonic contains quantum correction and that may be due to magnetic impurities or due to the presence of forward scattering. In our opinion it would be worthwhile to carry out further experiments in these directions, especially with magnetic impurities.

Summarizing the applicability of the present theory, the basic condition is that the CDW phase varies slowly in the Lee-Rice[9] domain and stronger phase deformations occur only in the immediate vicinities of the impurities. In this case the amplitude of the CDW order parameter is almost unperturbed except by the Friedel oscillations around the impurity. Under this condition the classical deformable CDW theory developed by Efetov and Larkin[8] and by Fukuyama, Lee, and Rice[9] can be applied on the length scale larger than the amplitude coherence length ξ_0, but in order to take into account the effect of Friedel oscillations around the impurities, an effective potential must be introduced for the impurity-CDW interaction in the Ginzburg-Landau equation. However, if the phase of the CDW changes rapidly near to the impurity but outside the region of the Friedel oscillations $x > x_0$, then the amplitude of the CDW must be reduced substantially around the impurity. For example, if the phase of the CDW were opposite on the two sides of the impurity just outside the region of the Friedel oscillations $(x_0 < x < \xi_0)$, then the CDW amplitude would vanish at the impurity site. This phenomenon is related to the ideas of Gor'kov[16] and of Ong, Verma, and Maki,[15] where phase-slip centers or vortices are discussed, and in an intermediate region the normal phase is formed.

ACKNOWLEDGMENTS

One of the authors (A.Z.) is grateful to John Bardeen for discussing the importance of the quantum processes in the CDW. The present work was very much initiated by the critical discussion of the previous Josephson theory with many physicists, especially with Daniel Fisher, P. A. Lee, G. D. Mahan, K. Maki, and C. M. Varma. Concerning the experimental situation we have benefited from discussions with G. Grüner, G. Mozurkewich, and P. Monceau. For discussions in all of the details of the present theory, we wish to thank L. P. Gor'kov and P. Nozières, who called our attention to the existence of the bound states, which are discussed in Sec. V. One of us (A.Z.) wishes to express his gratitude to S. E. Barnes, who initiated the previous work and to P. F. Tua, who participated in the early stages of the present work.

APPENDIX A

In Appendix B the time-dependent perturbation theory with adiabatic switching will be applied. The correlation functions appearing could be expressed in terms of Green's functions with several time arguments, but their analytical properties had to be taken carefully into account. In order to avoid these difficulties, the correlation functions will be calculated directly using the explicit form of the ground-state wave function. The ground-state

wave function $|0)$ is given in a form similar to the BCS wave function and the electron creation and annihilation operators will be expressed by quasiparticle operators of Bogolyubov type. In this appendix, the ground-state wave functions and the quasiparticle operators for the CDW will be listed.

The CDW is considered in mean-field approximation given by Eqs. (2.2) and (2.3). The Hamiltonian can be diagonalized by introducing the following quasiparticle operators,

$$\alpha_{-k,\sigma}=v_k e^{i\varphi_L}a^\dagger_{k,\sigma}+u_k e^{i\varphi_R}a^\dagger_{k+Q,\sigma}\ , \tag{A1}$$

and

$$\beta_{k,\sigma}=u_k e^{-i\varphi_L}a_{k,\sigma}-v_k e^{-i\varphi_R}a_{k+Q,\sigma}\ , \tag{A2}$$

where u_k and v_k are real and satisfy the identity

$$u^2_{k,\sigma}+v^2_{k,\sigma}=1\ . \tag{A3}$$

φ_R and φ_L are the phases of gauge transformation given by Eq. (2.10) and the momentum k runs over the left-hand side of the momentum space $-2k_F<k<0$. For the quasiparticle operators $\alpha_{-k,\sigma}$ and $\beta_{k,\sigma}$, the Fermi commutation relations holds.

The diagonalized form of the Hamiltonian (2.2) is

$$H_{\rm CDW}=\sum_{k,\sigma}E(k)(\beta^\dagger_{k,\sigma}\beta_{k,\sigma}+\alpha^\dagger_{-k,\sigma}a_{-k,\sigma}+1)\ , \tag{A4}$$

where the quasiparticle energy is

$$E(k)=\left[\Delta_0^2+\left[\frac{\epsilon_k-\epsilon_{k+Q}}{2}\right]^2\right]^{1/2}\ , \tag{A5}$$

and u_k and v_k are defined as

$$u_k=-\left[\frac{1}{2}\left[1-\frac{\epsilon_k-\epsilon_{k+Q}}{2E(k)}\right]\right]^{1/2}\ , \tag{A6}$$

and

$$v_k=\left[\frac{1}{2}\left[1+\frac{\epsilon_k-\epsilon_{k+Q}}{2E(k)}\right]\right]^{1/2}\ , \tag{A7}$$

and in case of linear dispersion $\epsilon_k=(\,|k|-k_F)v_F$ the term $\epsilon_k-\epsilon_{k+Q}$ has a simpler form $2v_Fp$ where $k=-Q/2+p$.

The ground-state wave function $|0)$ has the following simple form

$$|0)=\prod_{k\,(<0)}\alpha_{-k}|0\rangle\ , \tag{A8}$$

where $|0\rangle$ is the vacuum state. This ground-state wave function describes the free CDW by the build-in phase coherence between the states with momenta $p+Q/2$ and $p-Q/2$, furthermore, these state cannot be occupied simultaneously in the ground state.

The actions of the quasiparticle operators on the ground state are

$$\alpha_{-k,\sigma}|0)=\beta_{k,\sigma}|0)=0\ , \tag{A9}$$

$$\alpha^\dagger_{-k,\sigma}|0)=\prod_{\substack{k'\,(<0),\sigma\\ k'\neq k}}\alpha_{-k',\sigma}|0\rangle\ , \tag{A10}$$

and

$$\beta^\dagger_{k,\sigma}|0)=e^{i(\varphi_L+\varphi_R)}a^\dagger_{k,\sigma}a^\dagger_{k+Q,\sigma}\prod_{\substack{k'\,(<0),\sigma\\ k'\neq k}}\alpha_{-k',\sigma}|0\rangle\ . \tag{A11}$$

Finally, the expectation value of the electron density operator $\rho(x)=\sum_\sigma\psi^\dagger_\sigma(x)\psi_\sigma(x)$ in the ground state is

$$\rho^{(0)}(x)=s\sum_{k\,(<0)}(u_k^2+v_k^2)+2s\sum_{k\,(<0)}u_kv_k\cos(Qx-\varphi) \tag{A12}$$

which must be compared with Eq. (2.11) [see Eqs. (A5)–(A7) and Eq. (2.5)].

APPENDIX B

The force exerted on the CDW by the impurities has been calculated by Barnes and Zawadowski[13] using the linear-response theory where the interaction is switched on adiabatically. In their calculation the force is calculated up to second order of the perturbation theory and this method can be extended to higher orders. On the other hand, in Sec. VI the force is derived from the thermodynamical potential which is calculated in all orders of the perturbation theory. In order to show the equivalence of these two methods we are going to calculate the force in third order of the electron impurity interaction T by using both methods.

The electron-impurity interaction can be expressed in terms of the quasiparticle operators introduced in Appendix A and one obtains

$$\begin{aligned}H_{\rm imp}=&2Ts\cos\varphi\sum_{k\,(<0)}u_kv_k\\ &-\sum_{k,k',\sigma}g_1(k,k')(\beta^\dagger_{k,\sigma}\beta_{k',\sigma}+a^\dagger_{-k,\sigma}a_{-k',\sigma})\\ &+\left[\sum_{k,k',\sigma}g_2(k,k')\alpha_{-k,\sigma}\beta_{k',\sigma}+\text{c.c.}\right]\end{aligned} \tag{B1}$$

where

$$g_1(k,k')=Te^{i\varphi}v_ku_{k'}+Te^{-i\varphi}u_kv_{k'}\ , \tag{B2}$$

$$g_2(k,k')=Te^{i\varphi}u_ku_{k'}-Te^{-i\varphi}v_kv_{k'}\ . \tag{B3}$$

The first term of the Hamiltonian (B1) reproduces the result for the interaction energy in first order

$$E^{(1)}(\varphi)=-\frac{T\Delta_0}{\pi v_F\hat{g}}\cos\varphi\ . \tag{B4}$$

The corrections to the interaction energy are determined by calculating the thermodynamical potential,

$$\delta\Omega=-\frac{1}{\beta}(\langle S\rangle_c-1)\ , \tag{B5}$$

where

$$S=T_\tau\left[\exp\left[-\int_0^\beta H_{\rm imp}(\tau)d\tau\right]\right]\ , \tag{B6}$$

and, in terms of graphs, the index c means that only the connected diagrams have to be calculated. Using the

quasiparticle representation of the electrons, the thermodynamical potential $\delta\Omega$ can be calculated in the limit $\beta\to\infty$ in a direct way by taking the expectation value of the S matrix for the ground state and the integrals with respect τ can be carried out exactly. The results of these calculations are the following in the second and the third orders of the perturbation expansion:

$$E^{(2)}(\varphi)=-s\frac{T^2}{2}\sum_{k,k'}\frac{1-[\Delta_0^2/E(k)E(k')]\cos(2\varphi)}{E(k)+E(k')}\ , \tag{B7}$$

and

$$E^{(3)}(\varphi)=-\frac{sT^3}{2}\cos3\varphi\sum_{k,k',k''}\Delta_0^3\frac{1}{E(k)E(k')E(k'')}\frac{1}{E(k)+E(k')}\frac{1}{E(k)+E(k'')}$$
$$+s\frac{T^3}{2}\cos(\varphi)\Delta_0\sum_{k,k',k''}\left[\frac{1}{E(k)}+\frac{1}{E(k')}-\frac{1}{E(k'')}\right]\frac{1}{E(k)+E(k'')}\frac{1}{E(k')+E(k'')}\ . \tag{B8}$$

Following the method presented in Sec. VI the force can be calculated as the time derivative of the total momentum P of the electrons which is approximated by $P_{\rm app}$ introduced by Eq. (6.4). The expectation value of $\partial P_{\rm app}/\partial t$, at a given time t, can be expressed by the evaluation operator $U(t)$ as

$$\left\langle\frac{\partial P_{\rm app}}{\partial t}\right\rangle_t=\left\langle 0\left|U^\dagger(t)\frac{\partial P}{\partial t}U(t)\right|0\right\rangle\ , \tag{B9}$$

where

$$U(t)=T_t\exp\left[-i\int_{-\infty}^{t}H_{\rm imp}(t')dt'\right]\ . \tag{B10}$$

The expression of Eq. (B9) can be written as

$$\left\langle\frac{\partial P_{\rm app}}{\partial t}\right\rangle_t=\left\langle 0\left|\frac{\partial P}{\partial t}\right|0\right\rangle+i\int_{-\infty}^{t}dt'(0\,|\,[H_{\rm imp}(t'),\partial P/\partial t]_-\,|\,0)$$
$$+\int_{-\infty}^{t}dt'\int_{-\infty}^{t'}dt''(0\,|\,[[H_{\rm imp}(t'),\partial P/\partial t]_-,H_{\rm imp}(t'')]_-\,|\,0)\ . \tag{B11}$$

The operator $\partial P_{\rm app}/\partial t$ given by Eq. (6.6) can be expressed in terms of the quasiparticle operators as

$$\frac{\partial P_{\rm app}}{\partial t}=2TQs\sin\varphi\sum_k u_kv_k+iQ\sum_{k,k',\sigma}\{g_3(k,k')(\alpha^\dagger_{-k\sigma}\alpha_{-k',\sigma}+\beta^\dagger_{k\sigma}\beta_{k\sigma})-[g_4(k,k')\alpha_{-k\sigma}\beta_{k'\sigma}-\text{c.c.}]\}\ , \tag{B12}$$

where

$$g_3(k,k')=Te^{i\varphi}v_ku_{k'}-Te^{-i\varphi}u_kv_{k'}\ , \tag{B13}$$

$$g_4(k,k')=Te^{i\varphi}u_ku_{k'}+Te^{-i\varphi}v_kv_{k'}\ . \tag{B14}$$

A straightforward calculation leads to the following result:

$$\left\langle\frac{\partial P}{\partial t}\right\rangle_t=-Q\frac{T\Delta_0}{\pi v_F\hat{g}}\sin\varphi+QsT^2\Delta_0^2\sin(2\varphi)\sum_{k,k'}\frac{1}{E(k)E(k')}\frac{1}{E(k)+E(k')}$$
$$-\frac{3}{2}QT^3\Delta_0^3\sin(3\varphi)s\sum_{k,k',k''}\frac{1}{E(k)E(k')E(k'')}\frac{1}{E(k)+E(k')}\frac{1}{E(k)+E(k'')}$$
$$+QsT^3\frac{\Delta_0}{2}\sin\varphi\sum_{k,k',k''}\left[\frac{1}{E(k)}+\frac{1}{E(k')}-\frac{1}{E(k'')}\right]\frac{1}{E(k)+E(k'')}\frac{1}{E(k')+E(k'')} \tag{B15}$$

where the denominators $E(k)+E(k'')$ and $E(k')+E(k'')$ are the energy denominators of the perturbation theory and the expressions in front of them arise from the coherence factors $g_i(k,k')$ $(i=1$–$4)$. The time-ordered diagrams corresponding to the process considered here are shown in Fig. 15. The third-order diagram is just a correction to the second-order process in which one of the excited quasiparticles is scattered once more on the impurity.

The comparison of the results given by Eqs. (B7), (B8), and (B15) shows that the identity

$$\left\langle\frac{\partial P_{\rm app}}{\partial t}\right\rangle_t=-Q\frac{\partial E}{\partial\varphi} \tag{B16}$$

holds at least up to the third order in coupling T. This result supports the idea discussed in Sec. VII, that the calculations of the force F by switching the interaction adiabatically and by deriving from the static energy lead to the same expression.

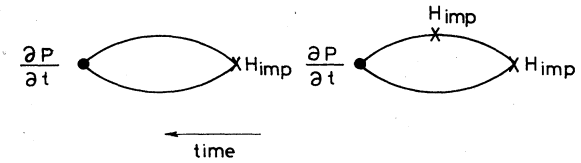

FIG. 15. Diagrammatic representation of the perturbation expansion of the time derivative of the total electron momentum P. The crosses represent the electron impurity interaction.

APPENDIX C

The basic approximation of the present calculations is that the interaction responsible for the formation of the CDW is taken into account in a mean-field approximation where the mean field $\Delta_0(\varphi)$ in Eq. (2.2) is not renormalized by the impurity scattering. The typical mean field diagram is depicted in Fig. 16(a) and the simplest renormalizations due to the impurity is shown in Fig. 16(b). Such renormalizations occur as a renormalization at the order parameter $\Delta(r)$ which has been calculated in Sec. III. In the following, the tendencies of these renormalizations will be investigated and the order of their magnitudes will be estimated.

A rough representation of the renormalized order parameter can be given by using Eqs. (3.33) and (4.9) in a simplified form

$$\Delta(r)=\begin{cases} 2D\,|\hat{g}|\left[\dfrac{T}{2v_F}\right]e^{-iQx}, & |x|<\dfrac{a}{2} \\ 2D\,|\hat{g}|\left[\dfrac{T}{2v_F}\right]\left[\dfrac{q/2}{x}\right]e^{-iQx}, & |x|>\dfrac{a}{2} \end{cases} \tag{C1}$$

which gives the correct features and orders of magnitudes for $T/2v_F<1$ in the region around the impurity where $\Delta(r)\gg\Delta_0$. The factor e^{-iQx} occurs because of the anomalous Green's function in the self-energy loop. The most drastic effect can be expected from the core part $|x|<a/2$ which shows strong resemblance with the impurity Hamiltonian given by Eq. (2.16), thus it can be taken into account as an additional term δT to the backward scattering amplitude T,

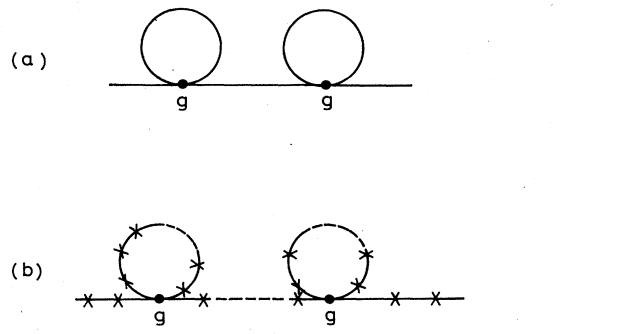

FIG. 16. Typical mean-field diagrams of the energy gap Δ. g represents the effective electron-electron interaction and the crosses represent the electron-impurity interaction. (a) shows a typical diagram without impurity while (b) shows the renormalization of the energy gap due to the impurity.

$$\delta T\sim 2D\,|\hat{g}|\left[\frac{T}{2v_F}\right]a\ , \tag{C2}$$

where $\Delta(r)$ is multiplied by the diameter a of the core region. This can be simplified by using the estimation $a/v_F\sim D^{-1}$ ($a/\hbar v_F\sim D^{-1}$) and one obtains

$$\delta T\sim\hat{g}T\ , \tag{C3}$$

thus the correction is small as $\hat{g}\ll 1$.

The tail of the renormalized order parameter given by Eq. (C1) can be considered as well, but the long-range part contributes only to the matrix element between electrons whose momentum difference is very close to Q. Thus the renormalization of the mean field by the impurity can be taken into account by a renormalization of the impurity backward scattering amplitude (strength and momentum dependence) but that renormalization factor cannot be very different from the unity.

[1]H. Fröhlich, Proc. R. Soc. London, Ser. A **233**, 296 (1954).
[2]P. Monceau, N. P. Ong, A. M. Portis, A. Meerschaut, and J. Rouxel, Phys. Rev. Lett. **37**, 602 (1976); N. P. Ong and P. Monceau, Phys. Rev. B **16**, 3443 (1977).
[3]R. Fleming and C. C. Grimes, Phys. Rev. Lett. **42**, 1423 (1979).
[4]R. M. Fleming, in *Physics in One Dimension,* Vol. 23 of *Springer Series in Solid State Sciences,* edited by J. Bernasconi and T. Schneider (Springer, Berlin, 1981); N. P. Ong, Can. J. Phys. **60**, 757 (1982); G. Grüner, Mol. Cryst. Liq. Cryst. **81**, 735 (1982); Comments Solid State Phys. **10**, 183 (1983). Other articles can be found in Proceedings of the International Symposium on Nonlinear Transport and Related Phenomena in Inorganic Quasi-One-Dimensional Conductors, Sapporo, Japan, 1983 (unpublished), p. 13, and in *Proceedings of the International Conference on Charge Density Waves in Solids,* edited by Gy. Hutiray and J. Soliyom (Springer, Berlin, 1985).
[5]G. Grüner, A. Zawadowski, and P. M. Chaikin, Phys. Rev. Lett. **46**, 511 (1981).
[6]P. Monceau, J. Richard, and M. Renard, Phys. Rev. B **25**, 931 (1982).
[7]P. Monceau, J. Richard, and M. Renard, Phys. Rev. Lett. **45**, 43 (1980).
[8]K. B. Efetov and A. I. Larkin, Zh. Eksp. Teor. Fiz. **72**, 2350 (1977) [Sov. Phys.—JETP **45**, 1236 (1977)].
[9]P. A. Lee and T. M. Rice, Phys. Rev. B **19**, 3970 (1979); H. Fukuyama and P. A. Lee; *ibid.* **17**, 535 (1978); P. A. Lee and H. Fukuyama, *ibid.* **17**, 542 (1978).
[10]L. Sneddon, M. C. Cross, and D. S. Fisher, Phys. Rev. Lett. **49**, 292 (1982); R. A. Klemm and J. R. Schrieffer, *ibid.* **51**, 47 (1983); D. S. Fisher, *ibid.* **50**, 1486 (1983) and Phys. Rev. B **31**, 1396 (1985); P. F. Tua and A. Zawadowski, Solid State Commun. **49**, 19 (1984); P. F. Tua and J. Ruvalds, *ibid.* **51**, 293 (1984); Leigh Sneddon, Phys. Rev. Lett. **52**, 65 (1984) and Phys. Rev. B **29**, 719 (1984); **29**, 725 (1984); P. B. Littlewood, in *Proceedings of the International Conference on Charge Density Waves in Solids,* Ref. 4, p. 369.

[11]J. Bardeen, Phys. Rev. Lett. **42**, 1498 (1979); **45**, 1978 (1980); Mol. Cryst. **81**, 1 (1981); in Proceedings of the International School of Physics, "Enrico Fermi", Varenna, Italy, 1983 (unpublished); Proceedings of the International Symposium on Nonlinear Transport and Related Phenomena in Inorganic Quasi-One-Dimensional Metals, Sapporo, Japan, 1983, Ref. 4 (unpublished), p. 1.

[12]J. Bardeen, in *Physics and Chemistry of Materials with Low-dimensional Structures, Series B: Quasi-One-Dimensional Structures,* edited by P. Monceau (Reidel, Dordrecht, 1983).

[13]S. E. Barnes and A. Zawadowski, Phys. Rev. Lett. **51**, 1003 (1983).

[14]K. Maki, Phys. Rev. Lett. **42**, 1498 (1979); Phys. Lett. **70A**, 499 (1979); Phys. Rev. B **18**, 1641 (1978); M. Weger and B. Horovitz, Solid State Commun. **43**, 583 (1982); Per Bak, Phys. Rev. Lett. **48**, 692 (1982).

[15]N. P. Ong, G. Verma, and K. Maki, Phys. Rev. Lett. **52**, 663 (1984).

[16]L. P. Gor'kov, Pis'ma Zh. Eksp. Teor. Fiz. **38**, 76 (1983) [JETP Lett. **38**, 67 (1983)].

[17]A. Zawadowski, I. Tüttő, S. E. Barnes, P. F. Tua, and J. Ruvalds, in *Proceedings of the International Conference on Charge Density Waves in Solids,* Ref. 4.

[18]J. Friedel, Philos. Mag. Suppl. **3**, 446 (1954) and Nuovo Cimento Suppl. **7**, 287 (1958).

[19]P. Monceau, M. Renard, J. Richard, M. C. Saint-Lager, H. Salva, and Z. Z. Wang, Phys. Rev. B **28**, 1646 (1983).

[20]M. P. Everson and R. V. Coleman, Phys. Rev. B **28**, 6659 (1983).

[21]P. F. Tua, A. Zawadowski, and J. Ruvalds, Phys. Rev. B **29**, 6525 (1984).

[22]A. I. Leggett, Ann. Phys. (N.Y.) **85**, 11 (1974).

[23]Yu. Bychkov, L. P. Gor'kov, and I. E. Dzyaloshinskij, Zh. Eksp. Teor. Fiz. **50**, 738 (1966) [Sov. Phys.—JETP **23**, 489 (1966)].

[24]L. P. Gor'kov and E. N. Dolgov, Zh. Eksp. Teor. Fiz. **77**, 396 (1979) [Sov. Phys.—JETP **50**, 203 (1979)], and J. Low Temp. Phys. **42**, 101 (1981).

[25]L. P. Gor'kov and O. N. Dorokhov, Fiz. Nizk. Temp. **4**, 332 (1978) [Sov. J. Low Temp. Phys. **4**, 160 (1978)].

[26]A. Zawadowski, Zh. Eksp. Teor. Fiz. **54**, 1429 (1968) [Sov. Phys.—JETP **27**, 767 (1967)].

[27]A. A. Abrikosov, L. P. Gor'kov, and I. E. Dzyaloshinskij, *Methods of Quantum Field Theory in Statistical Physics* (Prentice-Hall, Englewood Cliffs, 1963).

[28]P. Nozières (private communication).

[29]A. Zettl, thesis, University of California, Los Angeles, 1983.

[30]T. Tüttő (private communication).

[31]A. Zawadowski, J. Ruvalds, and J. Solana, Phys. Rev. A **5**, 399 (1972); A. Zawadowski, in *Quantum Liquids,* edited by J. Ruvalds and T. Regge (North-Holland, Amsterdam, 1978), p. 293.

[32]A. Zettl and G. Grüner, Solid State Commun. **29**, 755 (1984).

[33]S. E. Brown, G. Mozurkewich, and G. Grüner, Phys. Rev. Lett. **52**, 2277 (1984).

[34]See, e.g., Per Bak, in Proceedings of the International Symposium on Nonlinear Transport and Related Phenomena in Inorganic Quasi-One-Dimensional Conductors, Sapporo, Japan, 1983, Ref. 4 (unpublished) p. 13; M. Hogh Jensen, Per Bak, and T. Bohr, Phys. Rev. Lett. **50**, 1637 (1983); Per Bak, in *Statics and Dynamics of Nonlinear Systems,* edited by G. Benedek, H. Bilz and R. Zeyher (Springer, Berlin, 1983), p. 119.

[35]The observation of the subharmonics in $NbSe_3$ samples has been reported in Ref. 32 and in TaS_3 that was also observed by S. E. Brown, G. Mozurkewich, and G. Grüner, Solid State Commun. (to be published).

[36]Z. Z. Wang, M. C. Saint-Lager, P. Monceau, M. Renard, P. Gressier, A. Meerschaut, L. Guemas, and J. Rouxel, Solid State Commun. **46**, 325 (1983).

[37]G. Mozurkewich and G. Grüner (private communication).